We are IntechOpen, the world's leading publisher of Open Access books
Built by scientists, for scientists

6,900
Open access books available

186,000
International authors and editors

200M
Downloads

Our authors are among the

154
Countries delivered to

TOP 1%
most cited scientists

12.2%
Contributors from top 500 universities

CLARIVATE ANALYTICS
BOOK CITATION INDEX
INDEXED

WEB OF SCIENCE™

Selection of our books indexed in the Book Citation Index in Web of Science™ Core Collection (BKCI)

Interested in publishing with us?
Contact book.department@intechopen.com

Numbers displayed above are based on latest data collected.
For more information visit www.intechopen.com

4

High Performance Thermoplastic/Thermosetting Composites Microstructure and Processing Design Based on Phase Separation

Yuanze Xu* and Xiujuan Zhang
College of Chem. & Chem. Eng. Xiamen University, Xiamen,
Dept. Macromol. Sci. Fudan University, Shanghai,
China

1. Introduction

The merging of two research fields of thermoplastics and thermosets (TP/TS) is creating high performance composites with high rigidity, toughness and thermal stability etc. for versatile applications (Martuscelli,1996). However, most TP/TS mixtures do not always show the synergistic effects of rigidity and toughness as one expected (Bulknall, 1985; Douglas et al, 1991; Chen, 1995; Hayes et al, 200). On the other hand, the nature sets very elegant examples of strong solid structure, e.g. animal bones and wood plants, where sophisticated inhomogeneous structures are introduced to disperse the internal stress, yet keeping some interfacial strength to eliminating the micro-cracking or fracture propagation to achieve both high rigidity and toughness (Maximilien et al, 2010). Figure 1a is an example of SEM picture of animal bone, shown in Figure 1b is an illustrative example of a calculated bi-continuous phase separated structure of TP modified TS composites which resembles the nature occurring fine material structures.

This inspires us to improve the structures of our TP/TS systems, which will phase separate in a controllable way thermodynamically. Even very compatible mixtures of TP in TS matrices of practical importance will become incompatible during curing at certain stage, which is a prerequisite of toughening the brittle TS matrix. This process is so called cure reaction induced phase separation (CIPS) (Inoue 1995). CIPS provides an ingenious approach to realize controllable multi-scale phase morphology from nano-, micro to macro-scales (Hedrick et al, 1985; Ritzenthaler, et al, 2002a; 2003b), especially, the bi-continuous and/or phase inverted morphologies generated via spinodal decomposition may create some favorable structures which are critical in toughing the TS matrices (Cho,1993;Girard-Reydet et al, 1997; Oyanguren et al, 1999).

The separated phase morphologies will freeze through the matrix gelation or vitrification near Tg which become the final structures in TP modified TS composite materials. In this sense, our major task is to find some general relations between the miscibility, phase separated morphology evolvement, on one side, and the chemical structures of components and cure

* Corresponding Author

processing parameters in time-temperature windows on the other side. This is still a challenging goal up to now because of our limited knowledge of phase separation and the gaps between the CIPS research status and processing practices. To achieve the goal of morphology/process design, the combined efforts of multi-scientific approaches are employed both experimentally and theoretically on many practical systems of TP/TS/hardener. The results are promising as reflected in some of our recent publications (Zhang,2008;Zhang et al, 2008a;2007b;2008c;2006d;2006e) as well as in the new composite materials achieved based on this research for the structural parts of aircraft (Yi,2006;Yi et al, 2008;Yi & An,2008;Yi,2009).

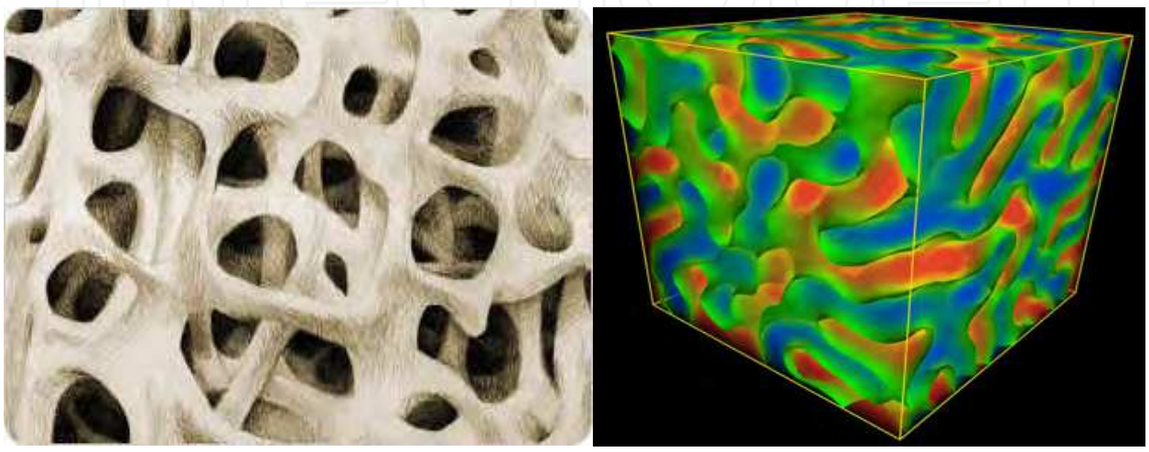

(a) (b)

Fig. 1. Skeletal structure of animal bone and simulated bi-continuous phase structure of some composite material. (a) Bone structure. (b) Bi-continuous phase of a composites in phase separation

The present chapter will provide a concise summary of our up-to-date original contributions with relevant literatures in this field emphasizing the breakthrough in approaches to understand and control the CIPS during processing.

2. Multi-scale design of the ideal composites

In macroscopic scale various reinforced TP or TS composites are designed with various graphite, glass and/other fibrous texture and alignments, where the matrices are treated as homogeneous. It is understood more and more that the rigidity and toughness of matrices are also of practical importance. The high rigidity & toughness require multi-scale controllable inhomogeneity of composites including bi-continuous and/or phase inverted micro-network with adjustable interface (Girard-Reydet et al, 1997; Oyanguren et al, 1999). After the concept of CIPS was proposed in 80s of last century (Inoue 1995), many experimental and theoretical investigations have been carried out to study the CIPS process in mixtures of tightly crosslinked TS matrices with ductile TP which is now assumed a promising alternative to rubber toughening approach, particularly when high value of elastic modulus, strength and glass transition temperature Tg are required.

For the continuous and/or inverse minor TP phase generated during CIPS and fixed in the thermosetting matrix, the most efficient toughening candidates are those that are able to

plastically deform and can withstand the crack bridging/pinning or crack deflection and yielding (Pearson & Yee, 1993). Proper adhesion between the interfaces of TP and TS phases is very crucial for effective toughening of the TS matrix. Poor adhesion will render the TP phase premature de-bonding before expected deformations occur, while over strong adhesion between TS and TP interface will restrain the extent of ductile deformation undergone by TP phase because of the excessive constraint brought by TS phase. This constraint would limit the amount of material which could be involved in the bridging and deformation process (Williams, 1997; Girard-Reydet et al 1997; Oyanguren et al, 1999). Therefore the modifier TP must be chose in such a way that optimal affinity between TP and TS components is ascertained properly whereby CIPS can occur freely while cracking and/or delaminating can be restraint. Good combination of TP/TS with proper miscibility and cure cycle can display synergistic toughening effect. Since the mechanical properties of the toughened materials are closely related to their final morphologies, many studies have been focused on the qualitative or pseudo-quantitative thermodynamic and kinetic analysis of the phase separation mechanism (Girard et al, 1998; Gan et al 2003;Zucchi et al,2004) and morphological microstructure control as we will describe in next sections. At the same time, lots of the researches on the CIPS are limited to academic concern, the control of the morphology during cure cycle of commercial application targeting predefined mechanical properties is to be disclosed.

The well studied process is to mix the high performance TP into the matrix to form a homogeneous solution of the two components, and the subsequent cure generates the phase separated morphological structures. This process is so called *in situ* approach, wherein the phase separated structures are distributed evenly in the matrix. Drawbacks of the *in situ* approach are the substantial increase of the matrix viscosity, whereby the handling and processing window of the composites are significantly deteriorated (Cheng et al, 2009) and, also, the adhesion and modulus match of TP/TS to strength reinforcer fiber may be not as good as TS alone. Contrary to the *in situ* toughing, *ex situ* toughing is an innovative concept of a spatially localized toughening concept (Yi et al), whereby the composites are fabricated by interleaving TP containing layers and TS impreged carbon fiber layers initially. During the CIPS and the interlaminar diffusion, formed a spatial gradient of toughness and rigidity between highly toughened layers to the non-toughened, high rigidity graphite plies. Thus, the basic idea of *ex situ* concept sets a good example of the multi-scale design by controlled processing. As a part of the *ex situ* manufacturing of composite, our work is focused on the CIPS morphology evolvement, chemorheology, the time-temperature dependence of CIPS process in broad time-temperature processing window with a combined approach of experiment and theory.

3. TP/TS miscibility & cure induced phase separation (CIPS)

3.1 Strategies and approaches

The curing process involves several transformation, e.g. from the viscous clear liquid to a phase separated opaque dope solution and then to three dimensional chemical gels, finally to a vitrified solid. Phase separation occurs due to the change of the mixing enthalpy and entropy which arise from the size increase of the thermosetting oligomers. Upon gelation,

the thermosetting systems lose fluidity permanently, and the phase domain loci are fixed, while the domains sizes keep growing through the component inter-diffusion. The gel times predefines the flowing operation window, e.g. the pot life, all the liquid molding methods such as RTM (resin transfer molding) have to be finished before permanent gelation. Vitrification is solidification that is defined to occur when Tg reaches cure temperature. Upon vitrification, the mobility of the composite molecules is restraint seriously, further polymerizations are restrained. So for TS composites processing, all the cure temperature usually are set above the material Tg for efficiency concerns. And the ultimate vitrification temperature set the material application temperature, once the environment temperature exceeds the material ultimate vitrification temperature, the material will become elastic rubber and the modulus and strength losses are serious, e.g. material yielding. To get material with desired morphology and properties, it is necessary to exploit these transformations to design the cure time-temperature processing routine so as to get the wanted ultimate structures and properties. In the following sections we describe the experimental approaches to detect and quantify the key parameters, from morphology to chemorheology in wide time/temperature space as presented by TTT (time–temperature-transformation) diagram (Grillet et al,1992; Simon & Gillham,1994). Our breakthroughs rely on the systematic studies on the phase separation time-temperature dependences during curing with the variations of the material parameters in a broad time/temperature space (Zhang et al, 2008a; 2007b; 2008c; 2006d; 2006e). To predict the possibility of various morphologies generated during cure, thermodynamic analysis based on Flory-Huggins-Staverman (F-H-S) theory was employed, which considers the free energy changing during demixing due to the enthalpy and entropy change during curing. It describes the spinodal and bimodal decomposition lines (Riccardi et al, 1994) while the relations to the structural parameters are to be clarified. Flory-Huggins-Staverman theory is widely used to describe the CIPS processes successfully in systems with UCST (up critical solution temperature) type phase behavior, like prediction the phase diagram together with the help of laboratory experiments of cloud point fitting (Riccardi et al, 1996; Girard et al, 1998; Ileana et al, 2004; Riccardi et al, 2004a; Reccardi et al, 2004b) and explain the morphology generated during cure, but further fundamental theoretical efforts are still needed. This is because at moment, the theoretical analysis is only successful for UCST systems, while those with LCST (lower critical solution temperature) type phase behavior are less well understood. The absence of property theoretical interpretation of LCST systems arises from the present theory approximation, wherein simplified assumption was made that the components are incompressible regarding to temperature, pressure and composition, while compressibility and special interaction place essential effect on the LCST phase diagram. The morphology evolution may be analyzed using time dependent Ginzberg- Landau equation (TDGL) of phase separation dynamics (Taniguchi & Onuki 1996) and the Viscoelastic model based on the fluid model(Tanaka 1997). Both models describe the morphological pattern evolvements, provides no clues yet about the temperature dependence of phase separation, though. All efforts towards processing condition will enable us better control CIPS and end-use properties of TP/TS composites.

In our present research, we focus on the curing systems which are widely studied and of great practical importance. Shown in Table 1 are chemicals we used throughout our study.

Abbreviations	Detailed chemical name	Chemical structure and characteristics
TGDDM	TGDDM: N, N, N', N'-tetraglycidyl-4, 4'-diaminodiphenylmethane, used as the matrix resin	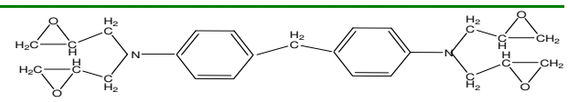
DGEBA	Diglycidyl ether of phenol A, used as the matrix resin	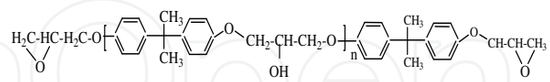
AroCyL10	Ethylidene di-4,1-phenylene ester, used as the matrix resin	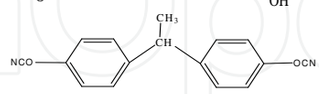
BMI	4,4′-bismaleimidodiphenylmethane, used as the matrix resin	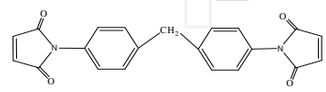
DBA	o,o′-diallyl bisphenol A, used as cure agent of BMI	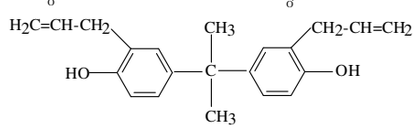
DDM	4,4′-diaminodiphenlyene methane, used as epoxy hardener	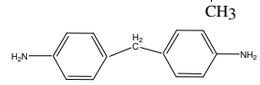
DDS	4,4'-diaminodiphenylsulfone, used as cure agent for epoxy resin	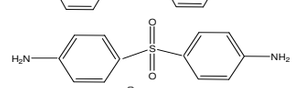
MTHPA	Methyl tetrahydrophthalic anhydride, used as epoxy hardener	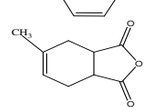
BDMA	Bipheylenemethylamine, initiator for the cure of DGEBA and MTHPA	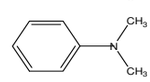
PEI	Poly(ether imide), used as modifier,	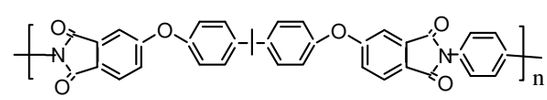
PEI1	Ploy(ether imide), used as modifier, provided by Prof. Shanjun Li	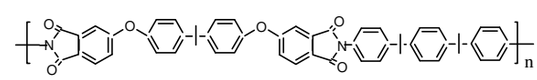
PES	Poly(ether sulphone) , used as modifier,	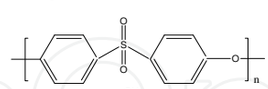
PSF	Polysulphone, used as modifier,	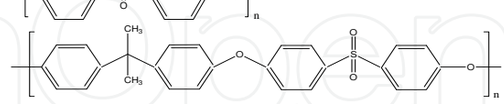
PES-C	Phenolphthalein poly(ether ether sulfone) , used as modifier,	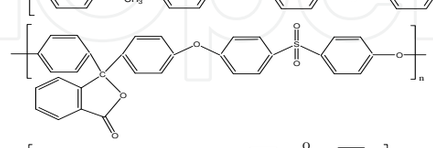
PEK-C	Phenolphthalein poly(ether ether ketone) , used as modifier,	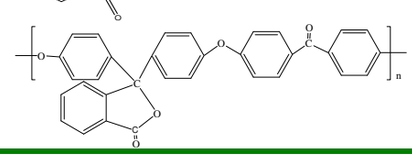

Table 1. Chemical structures of components employed in the present research

3.2 Detection of the cure induced phase separation process

The CIPS process can be observed in situ by different techniques, e.g. rheology (Xu et al, 2007; Zhang et al, 2006; Bonnet et al, 1999), small angle light scattering (SALS) and turbidity (Girard et al, 1998). Rheology can measure certain abrupt mechanical change upon phase separation, while SALS and turbidity trace the change of the optical mismatch between TP and TS rich domains during phase separation. SALS is most widely used to characterize the evolvement of domain size quantitatively in TP and TS blends (Bucknall & Gilbert, 1989; Girard et al, 1998; Gan et al 2003). In this work, we observed the early stage of CIPS in some TP/TS systems with a modified transmission optical microscope system(TOM) (Xu & Zhang,2007) and compared the microscopy method with the rheology and SALS approaches in the whole CIPS process. It was approved that the phase separation times can be determined by TOM. This enabled us to focus on the phase separation time/temperature dependence by considering the effects of TP molecular size and content, TP and TS structure, cure rate and cure mechanism and the stoichiometric ratio. The description of the whole cure time-temperature window of the thermoplastic modified thermosetting systems with the phase separation is of great importance in the composites processing industry.

3.3 Transmission optical approach

To observe the initial stage of phase separation, a lab-made computerized transmission optical microscope (TOM) system equipped with inversed optical design, long focusing objective lens and well controllable heating chamber was created which allows long term observation and data collection with a high resolution of 0.2μm in a wide working temperature range of RT~250°C (Xu & Zhang, 2007). The system can assign the onset of phase separation for systems with low refractive index difference and small domain size as low as 0.2μm, this won't be succeeded by usual TOM and SALS.

The samples for TOM observation were prepared by pressing the melt between two pieces of cover glass with a thickness of about 0.2mm. The moment when the morphological structure appeared was defined as the phase separation time t_{ps}. The values of t_{ps} at any particular temperature are the average of five measurements with observation errors of ±3% as measured in various TP modified TS systems (Zhang,2008; Zhang et al, 2008a, 2007b; 2008c; 2006d; 2006e).

We find that the phase separation times detected with different resolution optical lens are the same within a relative error of <±1.5% as shown in Table 2 for mixtures of DGEBA/DDM/PES and DGEBA/MTPHA/BDMA/PES with different PES content. The accuracy of the TOM approach to assign the onset of phase separation was also verified in various other systems like epoxy/DDS/PEK-C system, DGEBA/DDM/PEI, DGEBA/MTHPA/BDMA/PEK-C and (Cyanate ester)/TP systems. The fact that the t_{ps} values are independent on the magnification of the TOM proves that the onset of phase separation has been observed. If the initial phase domains were smaller than the resolution of the TOM system, one should see them earlier with higher magnification. The physical reason of limited initial domain size was explained as the nature of the cure induced spinodal decomposition by Inoue (Inoue, 1995; Ohnaga et al, 1994). Theoretically, the growing of TS size will drive the system into the unstable region in the phase diagram from

the stable state, which will result in the decreasing of concentration fluctuation wave length and the rising quenching depth theoretically. But the successive increase of the quenching depth has not changed the regular concentration fluctuation sine wave length at intermediate cure rate, as observed in most of the CIPS processes with spinodal decomposition, where very regular and fine bi-continuous or inverse phase separation were observed, computer simulation also verified such phenomenon. Possibly the increasing quenching depth depresses the domain coarsening arising from interfacial tension and hydrodynamics in the early stage of CIPS. Experimentally, in the initial stage of phase separation, the domain size keeps constant because of the compromising effect of domain coarsening and quenching increasing. So it seems no size variation appears in the early stage of CIPS, the concentration fluctuation wave length kept constant, and the limited value of initial fluctuation wavelength becomes the periodic size of phase domains in the early stage of phase separation before domain growth driven by interfacial tension and hydrodynamic force so the early stage of the spinodal decomposition can be observed at similar t_{ps} using different TOM magnification.

Mixtures	T/℃	t_{ps}/s (1500X)	t_{ps}/s (1200X)	t_{ps}/s (760X)	Error
DGEBA/DDM/PES 10ppm	163	94	92	93	-1-1%
	153	141	142	143	-0.7-0.7%
	143	209	206	207	-0.5-1%
	133	319	318	320	-0.3-.3%
DGEBA/DDM/PES 15ppm	163	88	89	87	-1.1-1.1%
	153	143	140	139	-1.4-1.4%
	143	178	178	177	-0.2-0.2%
	133	265	267	263	-0.8-0.8%
DGEBA/MTHPA/BDMA/PES 10phr	163	94	92	93	-1-1%
	153	141	142	143	-0.7-0.7%
	143	209	206	207	-0.5-1%
	133	319	318	320	-0.3-0.3%
DGEBA/MTHPA/BDMA/PES 15phr	163	88	89	87	-1.1-1.1%
	153	143	140	139	-1.4-1.4%
	143	178	178	177	-0.2-0.2%
	133	265	267	263	-0.8-0.8%

Table 2. Illustrative show of the effect of TOM resolutions on the phase separation times in TP/TS/hardener mixtures

3.4 Dynamic rheological measurements

The rheological experiments were performed with a rotational rheometer with disposable parallel plates (gap 1 mm and diameter 40 mm) (ARES of TA Instrument Co.). The multiple frequency dynamic time sweeps were conducted under the isothermal conditions using the time resolved rheometric technique to collect automatically multi-frequency data as function of time(Mours＆Winter,1994). The dynamic rheological data in Figure 2 were collected at frequencies 1, 2, 5, 10 and 20rad/s, respectively with an initial strain of 0.5 %. The strain level was automatically adjusted to maintain the torque response within the limit of the transducer.

Figure 2 shows the characteristic rheological profiles together with the corresponding morphological TOM micrographs of DGEBA/MTPHA/BDMA/PEK-C mixture along curing at 100^{0}C. There are two critical transitions in the plots of *tan δ* at different frequencies in the left layout in Figure 2. The curves cross at the times of phase separation t_{ps} and chemical gelation t_{gel} respectively, wherein loss tangent becomes independent of frequency and the dynamic modulus shows power law function with frequency (Chambon et al,1986; Hess et al, 1988). This critical status corresponds to the gel point and the network shows fractal structure, as we have discussed more systematically in previous work (Zhang,2008; Zhang et al, 2008; Zhang & Xu, 2006). It was found that the critical gel at phase separation exhibits lower fractal dimension, indicating the looser structure of TP network as will be explained in Section 4.

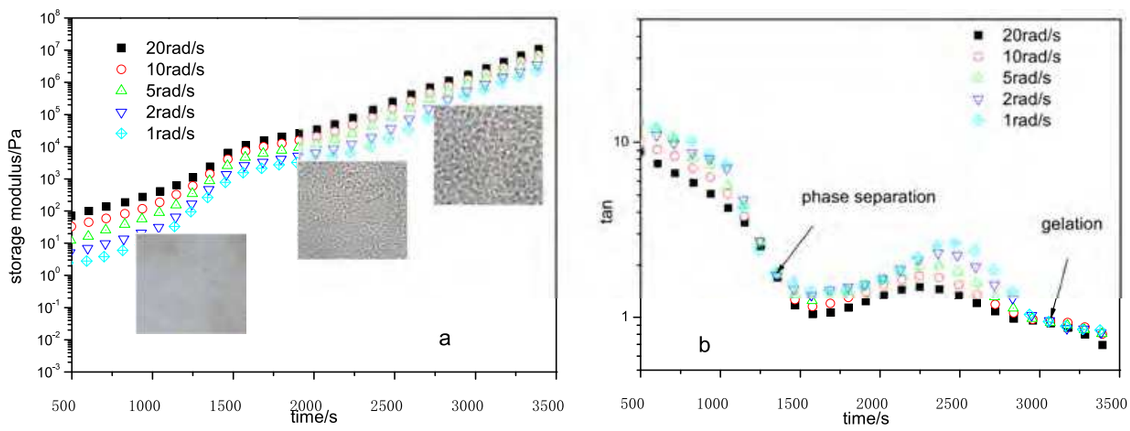

Fig. 2. Storage modulus G' (a) and tan δ (b) profiles and morphology evolvement of composite DGEBA/MTPHA/ BDMA/PEK-C 15phr systems cure isothermally at 100^{0}C

3.5 Small angel light scattering

The CIPS of systems with enough optical mismatches were observed *in situ* by SALS (small angel light scattering) using HeNe laser light (λ = 632.8 nm). Samples were mounted in a temperature controllable hot-stage. The scattering pattern generated by the sample was visualized on screen and recorded by a CCD. The time upon which the scattering ring appears is defined as the phase separation time. SALS is a good approach to monitor the structures in micron scale in size, wherein the phase separated structures have big enough optical mismatch (Girard-Reydet et al, 1998; Yu et al, 2004). SALS approach is unable in detecting the beginning time of phase separation process in some systems we studies like TGDDM/DGEBA/DDSPEK-C systems, whereas high resolution TOP and rheology take more effective role in characterizing the morphology evolvement (Zhang, 2008; Zhang et al, 2008; Zhang & Xu, 2006). Actually, the SALS method observes heterogeneous structures with sizes above micron (Girard et al, 1998), while the present TOM approach has an optical resolution of 0. 2μm and can concurrently give the direct morphology evolvement information.

It is interesting to have the CIPS systems with enough optical mismatches where the combined detection approaches can be employed giving the comprehensive *in situ* information. As shown in Figure 3a of the DGEBA/MTHPA/BDMA/PES system, the phase

separation time t_{ps} based on different observation means under various temperatures show a clear order: t_{ps} is earlier based on TOM, then rheology and SALS at last. In Figure 3b, DGEBA/MTHPA/BDMA/PEK-C shows similar sequential occurring between rheology and TOM approaches. It was observed that the phase separation time/temperature can be fit by the Arrhenius equation, whereby phase separation activation energy *Ea(ps)* was derived as shown in Table 3, which will be discussed in detail in the following sections. All the three approaches of SALS, rheology and TOM give slight different phase separation times, but the *Ea(ps)* in the two systems keeps almost constant, which was verified in lots of other TP modified TS systems. The discrepancy in the onset time of phase separation measured by different means probably comes from the fact that TOM detects smaller optical mismatch at initial stage of PS, while SALS needs sharper Interface and rheological measurement detects the overall mechanical response of the Components. Rheology is very very useful to get processing information.

Phase separation detecting means	PES 10phr		PEK-C10 phr		PEK-C15 phr	
	Ea(ps)/ kJ .mol^{-1}	R	*Ea(ps)*/kJ .mol^{-1}	R	*Ea(ps)*/ kJ .mol^{-1}	R
TOM	77.8	0.997	77.6	0.999	77.1	0.999
Rheology	75.8	0.999	78.3	0.999	77.1	0.999
SALS	76.7	0.999	/	/	/	/

Table 3. *Ea (ps)* values of DGEBA/MTHPA/BDMA/TP systems detected by different means

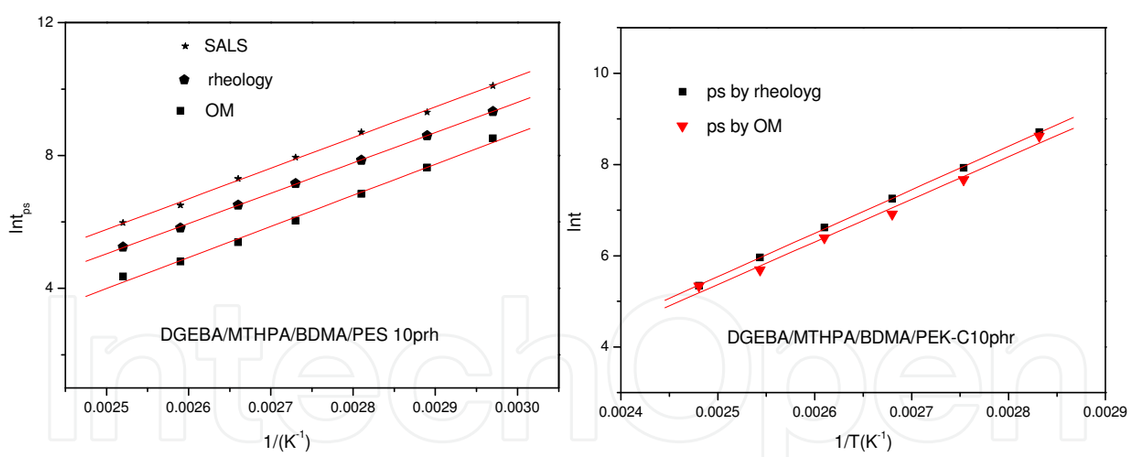

Fig. 3. Effect of detecting means on the time/temperature dependence for DGEBA/MTHPA/BDMA/TP systems

3.6 Differential scanning calorimetry

As a usual measurement method for TS curing study, DSC (differential scanning calorimetry) is a very convenient and effective means to monitor the thermosetting monomer cure kinetic, i.e. isothermal/dynamic cure rate, cure activation energy and cure enthalpy etc (Borrajo 1995; Bonnau, 2000). DSC is also widely used in the measurement of the polymeric material glass transition temperature Tg through the detection of heat capacity transition Cp

of the material during temperature scanning. In our present work, DSC technique is used to test the Tg of TS matrix and TP modifier, measure the cure kinetic at different temperatures and the cure activation energy *Ea*.

Figure 4 shows the dynamic exothermic and isotheral cure kinetic curves of DGEBA/MTHPA/BDMA/PEK-C10 with 0.45% initiator BDMA. As shown in the left layout, the temperature scanning curves of systems with different scanning rates. It can be observed that the peak temperatures vary with the change of scanning rate. Displayed in Figure 4b is the isothermal cure kinetics of DGEBA/MTHAP/BDMA/PEK-C10phr at 100°CBy fitting such cure kinetic curve, information about cure reaction order and cure activation energy etc can be got.

By making the temperature scanning of the raw material with different scanning rate, like 5, 10, 15, 20, 25°C/min, then analyze the exothermic curve and recognize the peak temperatures T_p, the cure activation energy is calculated as below:

$$Ea = -R * \frac{d\ln(\beta / T_p^{\,2})}{dT_p^{\,-1}} \tag{1}$$

Where β is the heating rate, *Tp* is the peak temperature, Ea is the cure activation energy and R is the gas constant.

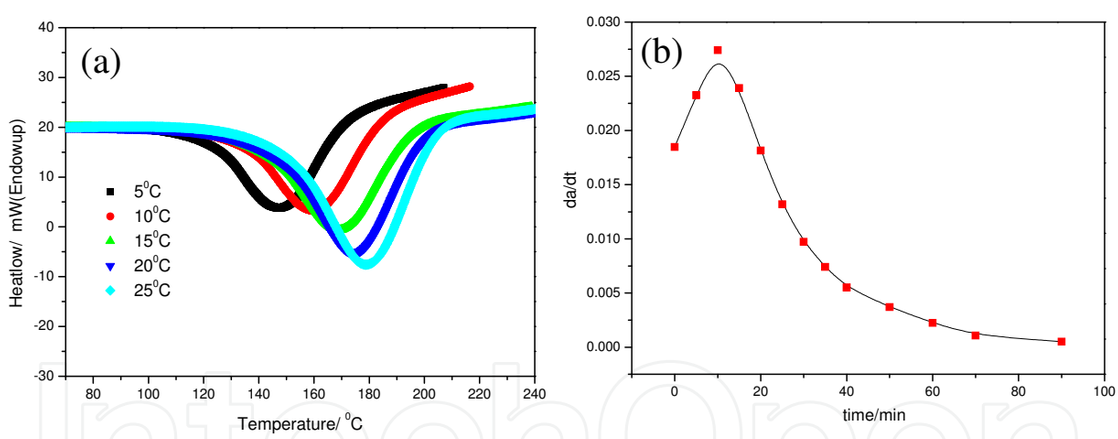

Fig. 4. DSC dynamic and isothermal cure kinetic monitor of DGEBA/MTHPA/BDMA/PEK-C10phr systems. (a) Exothermic curves. (b) Isothermal cure kinetics curve, r=1 at 100°C

4. CIPS of TP/TS in time-temperature window

4.1 Thermodynamic of CIPS process

Under the presence of TP, the cure reaction of thermosetting monomer with hardener is more complicated. According to the reaction mechanism, the polymerization of TS monomers falls into two groups: step polymerization and chain polymerization. Most TS monomers react via step polymerizations, which proceed by the stepwise reaction between the functional groups of reactive species wherein the size of the growing-TS molecules

increases at a relatively slow pace. Thus, different-sized species present in the reaction system and the large macromolecules appears only at the later stage of conversion with broadening molecular weight distribution. Thermodynamically, phase separation takes place because of the increase of molecular size of the TS component and possible change of the interaction energy between the TP and TS species. With the growing of TS in size, the entropy of mixing decreases which is a very critical contribution to the free energy of mixing. Besides the entropy change, the mixing enthalpy generated from the interaction energy variation, which may decreases and/or increases, relying on the specific interaction between TS and TP components. When the mixing free energy rise above zero, the system is driven into unstable region and spinodal phase separation takes place, bi-continuous or phase inverted phases precipitate. Usually, the phase separation, gelation and vitrification appear sequentially, i.e., the phase separation takes place prior to the chemical gelation and, finally, vitrification as Tg increases with crosslinking going on.

With this physical scheme in mind, the thermodynamics of the cure induced phase separation in TP modified TS systems could be approximated in the framework of Flory-Huggins lattice theory (Riccardi et al, 1996; Girard et al, 1998; Ileana et al, 2004; Riccardi et al, 2004a; Riccardi et al, 2004b):

$$\Delta g = RT\left(\sum_i \frac{\phi_{TS,i}}{iV_{TS,i}} \ln \phi_{TS,i} + \frac{1}{V_{TP}} \sum_j \frac{\phi_{TP,j}}{j} \ln \phi_{TP,j}\right) + B\phi_{TS}\phi_{TP} \tag{2}$$

Where Δg is the mixing free energy in unit volume, R is gas constant, T is absolute temperature $\Phi_{TS,I}$, $\Phi_{TP,j}$ are the volume fractions of TS_i and TP_j respectively, B the interaction energy density. There are two parts in eq. 2 dominating the direction of CIPS process. In the first part, the entropy decreasing with growing of TS in size is always favorable to phase demixing. The second factor comes from mixing enthalpy by the exchange interaction between TP and TS, it may increase with cure of TS (favoring demixing), or keeps constant throughout cure, or decrease with polymerization (favoring mixing). The second part in Δg is very crucial for the pattern of phase diagram, whereby various polymer combinations manifest different diagram, like upper critical solution temperature (UCST), lower critical solution temperature (LCST) and even combined UCST/LCST phase diagram. It should be mentioned that the interaction energy coefficient χ in Flory-Huggins theory framework is not an effective characteristic measure in describing CIPS process, since χ is only correlated with temperature, not enough for the description of TP modified TS with continuous changing of TS density. Because of the limitation of the theoretical framework, up to know, most of the thermodynamic analysis of the polymer phase separation phenomena are qualitatively discussed with the help of χ.

In present work, we study the phase separation time-temperature dependence on the chemical environment, which may arise from the stoichiometric imbalance and component structures variation. We will use interaction energy density parameter B as shown in eq. 2 instead of χ to explain the interesting phenomena ever observed widely in the TP modified TS systems. Based on the Hildebrand-Scatchard-van Laar（HSL）theory, the interaction energy density was defined as below:

$$B = \frac{\chi RT}{V_{ref}} \tag{3}$$

Where V_{ref} is a random reference volume. The interaction energy density B contains two parts, the first part is the energy coming from energy exchange during mixing of different components, the second part arises from other energy change, like the extra energy that generated from the incompressibility, hydrogen bonding etc. There are several approaches to calculate or estimate the interaction energy density B, such as experimental testing the binary phase diagram, then fitting the mixing diagram with certain theoretical equation; test the mixing energy with analogous chemicals and the estimation based on solubility parameters. Experimental determinations of the interaction energy density parameter B are very burdensome, sometimes difficult to do. In our present discussion, we will estimate B value by the solubility parameter approach. The solubility approximation simplifies the complex interaction energy expression between different components to the internal pure component interaction and inter-component interaction, by assuming that inter-component interaction is a geometric mean of each pure components interaction:

$$\delta_{TP/TS}{}^2 = \delta_{TP}\delta_{TS} \tag{4}$$

Where δ is Hildebrand solubility parameter and is defined as: $\delta = \sqrt{\frac{\Delta E}{V_m}}$, ΔE is the molar energy of vaporization, V_m is the molar volume (Hildbrand, 1950). So it is possible to calculate the B value through the solubility parameters δ_{TP}, δ_{TS} by equation:

$$B = (\delta_{TP} - \delta_{TS})^2 \tag{5}$$

For small molecules it is practical to test δ value directly by measure the enthalpy change during vaporization which is extensively tabulated. Considering the fact that the heat of vaporization of a macromolecule can not be measured experimentally, it is a common practice to calculate δ using the corresponding value of the solubility parameter of its monomers as substitute. Fedor, Van Krevelen et al.'s group additivity, computer simulation (Lewin et al, 2010) and thermodynamic analysis (Fornasiero et al, 2002; Utracki & Simha, 2004) are also used widely in literature. Bicerano (Bicerano, 2002) developed a topological approach to calculate δ values based on the interaction index method, whereby group contribution is not necessary, δ can be deduced based on the polymeric chemical structure. We will illustrate the basic process to calculate δ as follow.

First, draw the skeletal structure of MTHPA in Figure 5a:

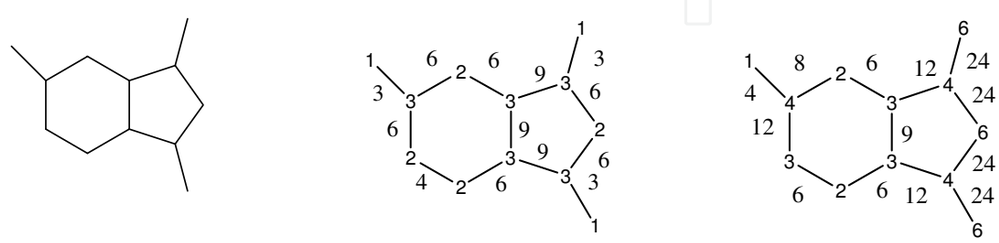

(a) (b) (c)

Fig. 5. (a) Hydrogen suppressed graph obtained by omitting the hydrogen atoms and connecting all of the remaining atoms (vertices of the graph) with bond(edges of the graph)

Then based on the simple atomic index γ of skeletal structure, non-hydrogen vertexes and the atom valence index γ^v to calculate the bond index $\beta_{ij} = \gamma_i * \gamma_j$ and valence index $\beta^v{}_{ij} = \gamma^v{}_i * \gamma^v{}_j$, the zero order connection index ${}^0\xi \equiv \sum_{vertices} (\frac{1}{\sqrt{\gamma}}) = \frac{3}{\sqrt{1}} + \frac{4}{\sqrt{2}} + \frac{5}{\sqrt{3}}$ =8.72 and ${}^0\xi^v \equiv \sum_{vertices} (\frac{1}{\sqrt{\gamma^v}}) = \frac{1}{\sqrt{1}} + \frac{2}{\sqrt{2}} + \frac{3}{\sqrt{3}} + \frac{3}{\sqrt{4}} + \frac{3}{\sqrt{6}}$ =6.87 and the first order connection index $\xi^1 \equiv \sum_{vertices} (\frac{1}{\sqrt{{}^1\beta}}) = \frac{3}{\sqrt{3}} + \frac{1}{\sqrt{4}} + \frac{6}{\sqrt{6}} + \frac{3}{\sqrt{9}}$ =5.68 and ${}^1\xi^v \equiv \sum_{vertices} (\frac{1}{\sqrt{{}^1\beta^v}})$ =4.09. Then put the connection index into equation for volume $V=3.64*{}^0\xi+9.799*{}^0\xi^v-8.54*{}^1\xi+21.69*{}^1\xi^v+0.98*N_{MV}$ (N_{MV} correction item) and cohesion energy $E_{Fedor}\approx 9882.5*{}^1\xi+358.7*(6*N_{atomic}+5*N_{group})$($N_{atom}$ and N_{group} correction)：$\delta = \sqrt{\frac{E_{coh}}{V}}$ =21.8 $J^{1/2}/cm^{3/2}$. Then put δ into eq.4 to obtain B value. In our following discussion, all the interaction energy density parameters B are calculated based on Bicerano's approach.

4.2 Rheological characterization of the CIPS process in TP/TS mixture

TS/TP/harder is a typical asymmetric mixture. Most TP systems which are of practical importance usually have much higher molecular mass, higher modulus and Tg than that of TS monomers. The large difference in modulus/Tg and molar mass of TS and TP are responsible for the dynamical asymmetry in the relaxation and diffusion of chain which play a critical role in the early stage of phase separation process (Gan et al, 2003;Yu et al, 2004). At the beginning, TP was dissolved in the TS monomers homogenously. With cure going on, TS grows in size and the storage modulus built up higher as shown in Figure 2. When the miscibility between TP and TS jumped into the unstable region, TP precipitated out as inverse phase, or as nodular or dispersed phase depending on the TP volume fraction. The phase separation process is manifested by the abrupt increases of viscosity and modulus profiles. Then the viscosity and modulus evolve further upwards, which grow in a step way in the chemical gelation vicinity again. As can be found that phase separation occurs before chemical gelation - the infinite TS molecular structures originated from the percolation of the TS oligomers. As displayed in Figure 2b, two critical gel points were found, the first one occurs at the phase separation time t_{ps} which was verified by the morphological observation by TOM, the second critical gelation phenomenon appears at the chemical structure percolation point t_{gel} which was confirmed based on DSC isothermal exothermic process, solubility test and rheological study of the neat TS cure process (Macosko & Millerlb,1976).

It was observed in the beginning of cure, the TP/TS/harder blends have a storage modulus G' much lower than the loss modulus G″, which implies the viscous essentiality of the homogenous mixtures. Upon curing, G' grows in a more steep manner than G″. At the vicinity of phase separation point t_{ps}, log-log plots of G' and G″ versus ω became parallel and the loss angel factor tanδ became independent on frequency, implying a critical gel transition. TOM proved the appearance of the bi-continuous phase structure at this first

transition. As the reaction proceeds, the shape of G' plots is further altered by the second rapid increase of G' which corresponds to the chemical gelation of TS oligomers confirmed by solubility tests and rheological monitoring on neat TS cure. After gelation, the margin of the domains became clearer gradually due to further phase separation and the coarsening of phase pattern can be observed depending on the interfacial tension and the viscosities of the phases.

4.3 The critical gel behaviors at t_{ps} and t_{gel}

As shown in Figure 6, at the vicinity of phase separation point t_{ps} and chemical gelation point t_{gel}, G' and G″ involve in a parallel manner versus frequency ω in log-log plot, while loss angel factor tanδ become independent on frequency, implying the characteristic gel transitions, which Winter et al named as critical gel state (Scanlan & Winter, 1991). We will discuss such critical gel behaviors and its applications more systematically in following sections.

At both t_{ps} and t_{gel}, the dynamic scaling behaviors of storage modulus G' and the loss modulus G'' appears as shown in Figure 6, where G' and G'' versus frequency in the vicinity of t_{ps} and t_{gel} for system of DGEBA/MTHPA/BDMA/PEK-C 15phr isothermally curing at 100°C are displayed, the curves have been shifted horizontally by a factor A (see insert) for easier comparison. As can be seen G' and G'' show a power low relation through eq.6；

$$G' \propto G'' \propto \omega^n \tag{6}$$

Where ω is frequency; n is the critical relaxation index.

The difference between the critical gel at t_{ps} and t_{gel} was noticed that G' is less than G'' at t_{ps} while larger than G'' at t_{gel} as shown in Figure 6 and also reported in other systems (Scanlan & Winter, 1991). The second difference is in the slop of log G', G'' vs. log ω curves at critical states. The critical gel index at both of t_{ps} and t_{gel} are calculated and summarized in Table 4 for DGEBA/MTHPA/BDMA/PEK-C system with PEK-C of 15, 10, 5phr respectively. The scaling behaviors occur at both t_{ps} and t_{gel} and over the entire experimental temperature range of 90~130°C.

By analyzing the data in Table 4, it can be found that both of n_{ps} and n_{gel} are independent to cure temperatures within the experimental range, more significantly, n_{ps} is reasonably larger than n_{gel}. The existence of the power law index n value for a critical gel is a signature of its structure of self-similarity, for which the fractal geometry can be applied. Based on percolation theory, Muthukamar suggested that, the fractional dimension d_f can be represented in terms of power law index (Muthukumar, 1989):

$$d_f = \frac{(d+2)(d-2n)}{2(d-n)} \tag{7}$$

Where d_f is the fractal dimension and d is the space dimension.

Taking the values of n_{ps}, n_{gel} and space dimension of 3 to eq. 7, we obtained the value of fractional dimension at phase separation point $d_{f,ps}$ and chemical gelation point $d_{f,gel}$

respectively, both of which are summarized in Table 4. As was observed that bigger n gives a smaller fractional dimension implying looser crosslinking network. The values of $d_{f,gel}$ are within the range of most single TS gelation, as reported in the other networking systems (Eloundou,1996). The PS network is clearly looser than the chemical gelation ones. The TS crosslinking expels the less mobile high mass TP to form a sponge-like loose structure, where physical entanglement of TP macromolecules appears, causing storage modulus G′ jump or tangent loss drop. This may explain why the phase separation dimension fractional $d_{f,ps}$ values increase with the increase of TP content. It is also noticed that the chemical gelation factional dimension $d_{f,gel}$ also increases with the increase of TP content. The explanation may not be easy since multi-factors involved in the cure process with PS: component diffusion mobility, interface stability, hydrodynamic effect and the competition between phase separation dynamics and crosslinking mechanism (stepwise or chainwise polymerization) etc.

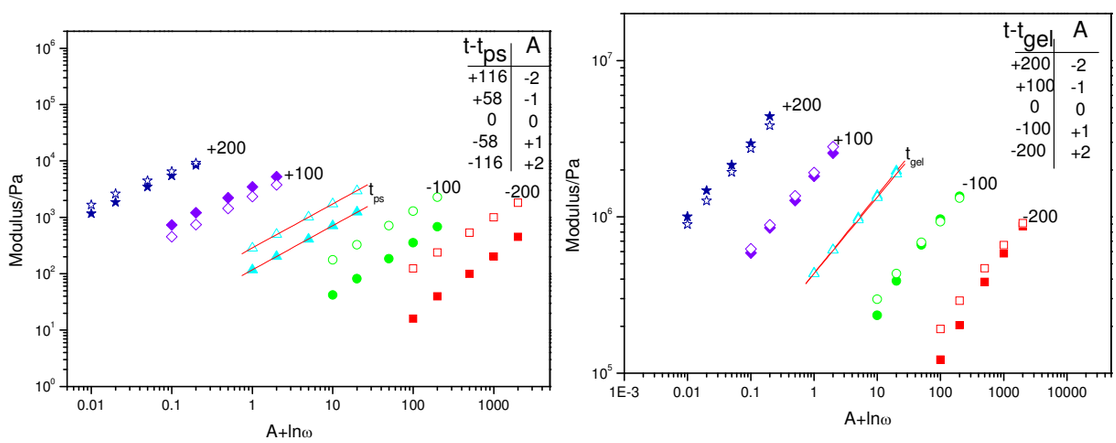

Fig. 6. Frequency response of G' (the solid symbols) and G'' (the open symbols) at the vicinity of t_{ps} and t_{gel} for DGEBA/MTHPA/BDMA/PEK-C 15 phr cure under 100°C

Temperature /°C	PEK-C 15phr				PEK-C 10phr				PEK-C 5phr	
	n_{ps}	$d_{f,psl}$	n_{gel}	$d_{f,gel}$	n_{ps}	$d_{f,psl}$	n_{gel}	$d_{f,gel}$	n_{gel}	$d_{f,gel}$
130	0.65	1.81	0.43	2.08	0.81	1.58	0.54	1.95	0.78	1.62
120	0.68	1.77	0.48	2.02	0.83	1.54	0.52	1.98	0.78	1.62
110	0.78	1.62	0.47	2.04	0.80	1.59	0.52	1.98	0.79	1.61
100	0.78	1.62	0.50	2.00	0.76	1.65	0.54	1.95	0.79	1.61
90	0.71	1.72	0.50	2.00	0.83	1.54	0.50	2.00	0.77	1.64

Table 4. Power law index at t_{ps} and t_{gel} under different temperatures for DGEBA/MTHPA/BDMA/PEK-C system

It is understood that the phase separation is incomplete after t_{ps} and some second component still left in the TP or TS rich phase for thermodynamic or kinetic reason. When the TP chain length is long enough like PEK-C we used in our study with molecular size far beyond the entanglement limit size, TP will behavior in such a way that the more the TP exists in TS rich phase, the denser the gel network will be. Similar scenarios can be imaged in the TP rich phase. Based on the kinetic and hydrodynamic approaches, we can explain the second phase separation observed usually in the CIPS process as was illustrative displayed in Figure 7, where TP and TS rich phase contain second phase respectively (Oyanguren et al, 1999). Here DGEBA reacts with hardener MTHPA at the presence of initiator BDMA through the chain polymerization, wherein large quantities of monomers exist upon phase separation, which will contribute greatly to the interface instability, second phase separations were observed in different temperature at different PEK-C contents as displayed in Figure 7a and Figure 7b. Low molecular weight TP show strong mobility after t_{ps}, also enhance the domain coarsening and second phase separation.

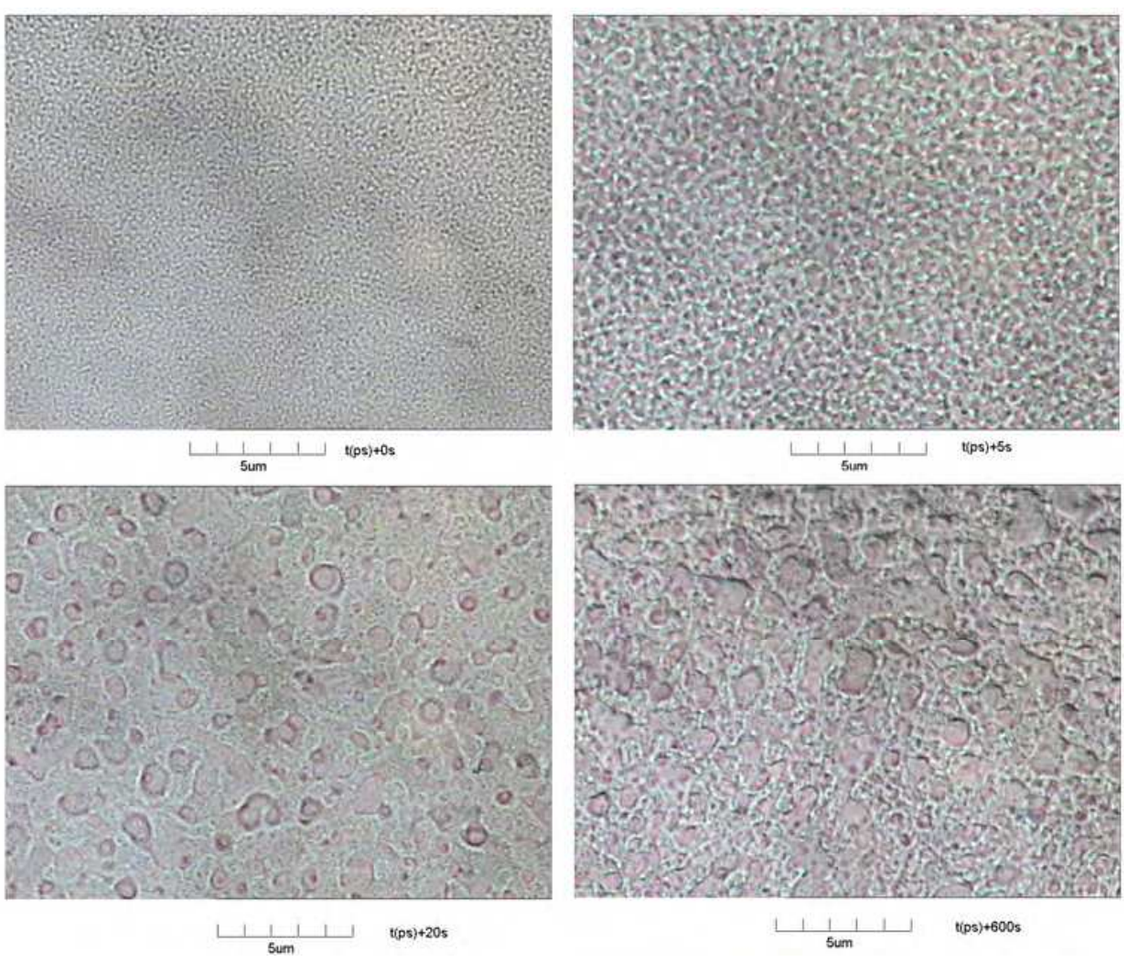

(a)

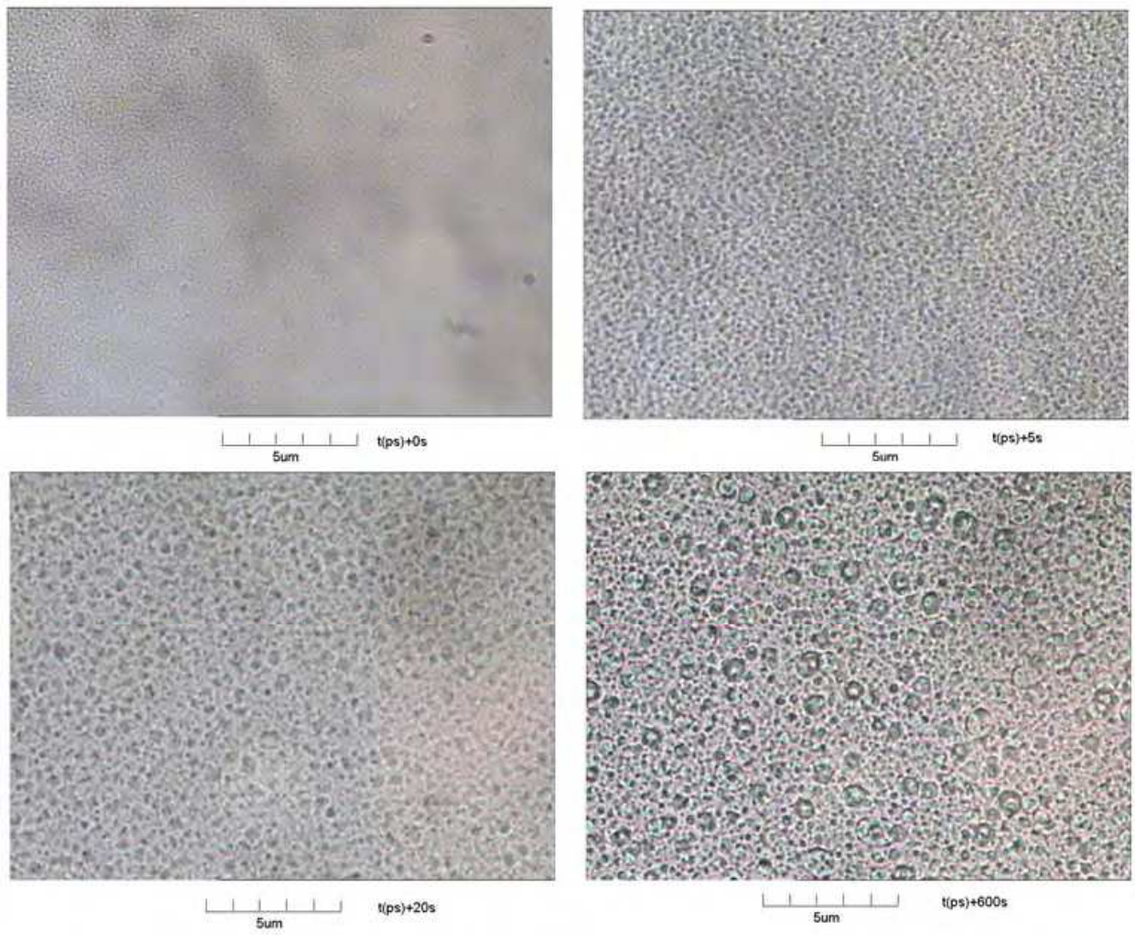

(b)

Fig. 7. Morphology evolvement of DGEBA/MTPHA/BDMA/PEK-C with different PEK-C content at 100°C (a)DGEBA/MTHPA/BDMA/PEK-C10prh
(b) DGEBA/MTHPA/BDMA/PEK-C 15prh

The critical phenomena during the CIPS process in other TP modified TS system were also observed, e.g. cyanate ester Arocy L-10/$Cu(Ac)_2$, DGEBA/DDM/PES and TGDDM/DGEBA/DDS/PEK-C systems etc.

5. Processing of TP/TS in time-temperature window, TTT diagram

5.1 Cure induced phase separation time-temperature dependence

Based on the determination of the phase separation times in different TP/TS/hardener systems at different temperature, we are able to study its temperature dependency. It was found that cure induced phase separation time & temperature relation fits into the Arrhenius form, irrespective the observation approaches of rheology, TOM or SALS:

$$\ln t_{ps} = \ln k + \frac{Ea(ps)}{RT} \tag{8}$$

Wherein t_{ps} is the phase separation time, *Ea(ps)* is the phase separation activation energy, *T* is the absolute temperature, and *R* is the universal gas constant.

The Arrhenius type dependence of CIPS time & temperature was observed in a various TS/TP/hardener mixtures, including the UCST (up critical solution temperature) and LCST(low critical solution temperature) types mixtures. The phase separation processes were monitored with TOM and rheology, some of them were also observed with SALS techniques. As were shown in Figure 3 and Table 3, the phase separation time-temperature dependency represented by phase separation activation energy *Ea(ps)* is independent on the detection means. The generality and factors which impair influence on *Ea(ps)* values have been discussed in detail in our published/unpublished works (Zhang,2008;Zhang et al, 2008a;2007b;2008c;2006d;2006e). It was observed that *Ea(ps)* values relay on the TP/TS internal chemical environment, like TS cure stoichiometric ratio, chemical structures of TP and TS, cure activation energy *Ea* etc, while the TP content, TP molecular size and cure rate show no obvious effect on the value of *Ea(ps)* in the TP/TS systems as far as TPs were employed as the minor part to toughen the TS matrix and cure reaction kinetics follows the Arrhenius type temperature dependence. Illustrative explanation on the time-temperature dependence of the CIPS in TP modified TS systems are made as following subsections.

5.2 Effect of TP contents and TP molecular size on *Ea (ps)*

Based on comprehensive study of the CIPS process of various TP/TS combinations in our research group, it was found that the phase separation energy *Ea(ps)* is independent on the TP content, wherein the TP is the minor modifier to toughen the TS matrix, systems with TS as minor component used as plasticizer are out of the scope of our research.

Illustratively Shown in Figure 8 are the drawings of $\ln t_{ps}$ vs. *1/T* for the LCST type system DGEBA/MTHPA/BDMA /PEK-C and UCST type system Cyanate ester AroCyL10/accelerator/PEI with different TP contents, respectively. The corresponding phase separation activation energy values of *Ea(ps)* derived from the slope of the $\ln t_{ps}$ vs. *1/T* plots are summarized in Table 5. As depicted in Figure 8, although both of the two systems contain different TP contents, phase separation times t_{ps} can be well correlated with cure temperature in Arrhenius type in wide cure reaction temperature. The *Ea(ps)* values shown in Table 5 are not sensitive to the TP content within the experimental range. The independency of *Ea(ps)* on the TP level can be understood from the physical origin of the CIPS process. Although the starting TP levels are different for the studied systems, but the driving force, and the chemical kinematics are same, which is manifested by the similar activation energy *Ea.*

Similar trends were also observed in other systems, e.g. Epoxy/anhydride/Initiator/PES (PEI) systems, Epoxy/amine /PES(PEI) systems, Epoxy/amine/PEK-C systems, Cyanate ester (AroCyL-10)/catalyst/PES system and Bismaleimide /TP systems. In all these systems, the phase separation times may vary because of the phase separation detection means, but the Arrhenius type phase separation time/temperature dependency Keeps unchanged. The exceptions could be mentioned that at high enough TP contents, the chemical reaction kinetics will be restraint because the high viscous environment will hinder the molecules free diffusion, under such event, Arrhenius type cure kinetic is not applicable,

or when the cure temperature near glass temperature, diffusion incorporated model is necessary (Kim,2002).

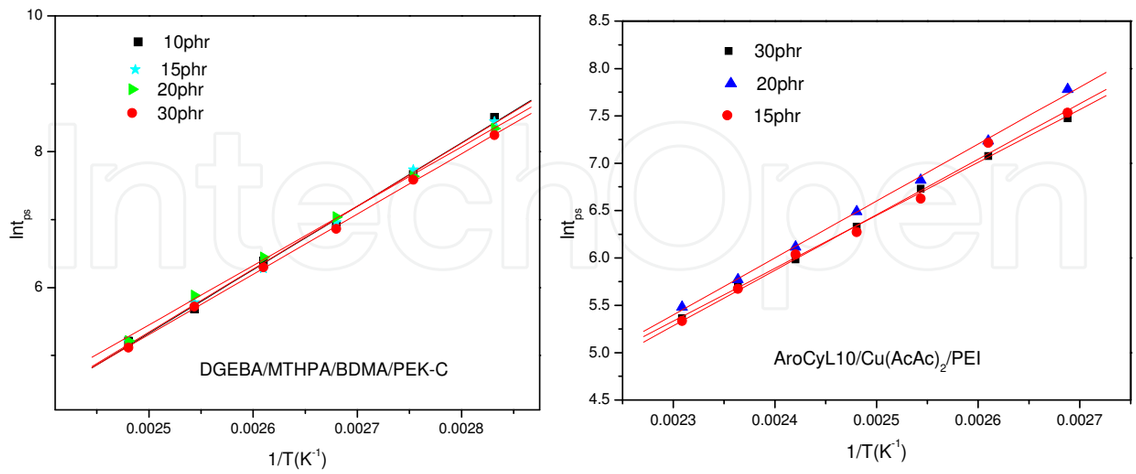

Fig. 8. Effect of TP content on the relation of $\ln t_{ps}$ *vs.* $1/T$ of DGEBA/MTHPA/BDMA/PEK-C and (AroCyL10) / $Cu(AcAc)_2$/PEI systems

TP content /phr	DGEBA/MTHPA/BDMA/PEK-C				(AroCyL10)/ $Cu(AcAc)_2$/PEI			
	Ea(ps, TOM)/ kJ .mol^{-1}	R	*Ea*/kJ .mol^{-1}	R	*Ea(ps, TOM)*/ kJ .mol^{-1}	R	*Ea*/kJ .mol^{-1}	R
5	77.1	0.999	73.3	0.999	n.d.	n.d.	60.1[a]	0.999
10	77.6	0.999	73.7	0.999	47.9	0.998	59.2	0.999
15	77.1	0.999	n.d.	n.d.	48.5	0.999	n.d.	n.d.
20	76.6	0.999	73.4	0.998	47.8	0.999	60.1	0.999

a: The reaction activity energy of both neat thermosetting monomer were determined by the gel point method

Table 5. *Ea(ps)* of DGEBA/MTHPA/BDMA/PEK-C and (AroCyL10)/$Cu(AcAc)_2$/PEI with different TP content

To understand the effect of the TP content on the component chain mobility and cure activation energy, the chemorhelogical processes of some TP modified TS systems were analyzed. The following chemorheological relationship (Halley & Mackay,1996) is applied to the TP/TS system with cure.

$$\ln \eta(t) = ln\eta_0 + kt \tag{9}$$

Wherein η_0 the initial viscosity of the system without curing，k reaction kinetic constant which is dependent to reaction temperature and cure reaction kinematic constant,η_0 and k follow Arrhenius form equation：

$$\eta_0 = \eta_\infty \exp\frac{E_\eta}{RT} \tag{10}$$

$$k = k_{\infty} \exp \frac{E_k}{RT} \tag{11}$$

The cure reaction process accompanied by the phase separation process of the TP modified TS systems with different TP content was monitored, the viscosity evolvement before phase separation was fitting by the Arrhenius chemorheological relation. Illustratively shown in Figure 9a are the complex viscosity η* profiles of DGEBA/MTHPA /PEK-C10phr with 0.9% initiator BDMA just before phase separation in the linear coordinate, displayed in Figure 9b is the same data but in the semi-log coordinator. The complete η* profiles under different cure temperature were displayed in the up right corner of Figure 9a. In Figure 9b of the semi-log coordinate, the η* curves were shifted on purpose by a factor of A, which is denoted by the number beside each curve. The straight forward trends of each curve in the semi-log coordinate imply that the cure process can well be fitted by the Arrhenius relationship. The cure activation energy E_k and viscous flow energy E_η were calculated and summarized in Table 6 respectively. It can be found in the present TP loading levels, E_k and E_η keep constant with the varying TP content. The results were confirmed in other characterization approaches, e.g. gelation and exothermic methods and in other systems. Flow viscosity itself is sensitive to the dragging effect exerting by TP macromolecules, while the viscous activation energy E_η value is related to smaller scale of TP chain segments. Considering the related mechanisms of E_η and *Ea (ps),* it is understandable that *Ea(ps)* keeps constant regardless the variation of TP content in low TP contents. The constant E_η values of the systems with different PEK-C loading level indicate that TP has no effect on the diffusion mobility of the TS oligomers during phase separation.

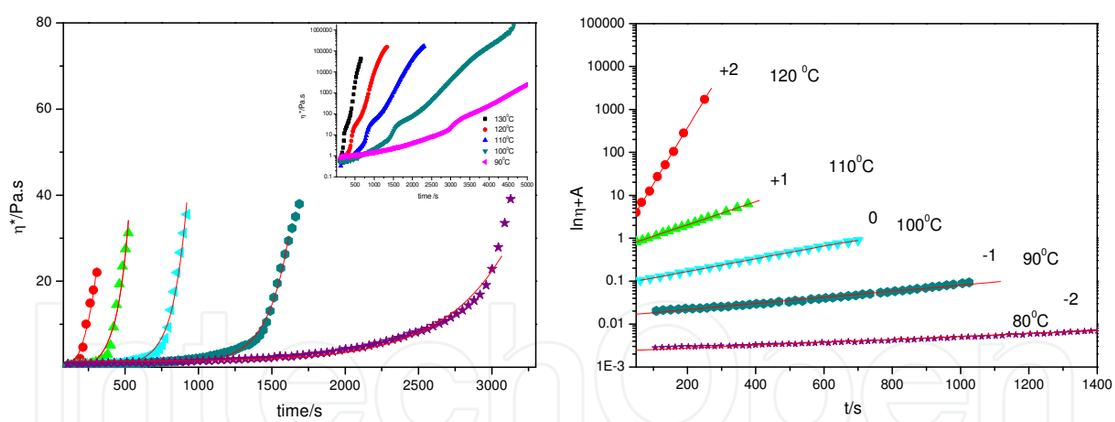

(a) (b)

Fig. 9. Viscosity profiles of DGEBA/MTHPA/BDMA/PEK-C10ph system prior to phase separation under different cure temperatures. (a) η* profiles before t_{ps} in linear coordinator. (b) η* before t_{ps} in semi-log coordinator

PEK-C contents/phr	E_η/kJ .mol^{-1}	E_k/kJ .mol^{-1}	*Ea(gel, rheology)* / kJ .mol^{-1}	R
10	21.9	76.7	78.3	0.999
15	24.8	78.7	77.1	0.999
20	20.8	77.7	76.6	0.999

Table 6. E_η and E_k values of DGEBA/MTHPA/BDMA/PEK-C systems with different PEK-C content, BDMA content 0.9%

Shown in Table 7 are the phase separation time-temperature dependences of DGEBA/MTHPA/BDMA/PEK-C and DGEBA/MTHPA/ BDMA/PES systems with TP of difference molecular size, depicted by the intrinsic viscosity of [η]. It was observed that the $E_a(ps)$ are not altered obviously by the variation of TP molecular size. Theoretically, the miscibility of TP/TS changes with the size of TP as disclosed by Buckanall (Bucknall et al, 1994) in DGEBA/PES systems, which may change the startup of phase separation times t_{ps}, but the chemical reaction kinetics has not been altered significantly as shown in Table 7 denoted by cure activation energy *Ea,* wherein the effect of the variation of TP content resembles the effect of TP molecular size effect. In fact we found that some of the phase separation time/temperature data in published in literatures also followed the Arrhenius equation, e.g. from the data based on turbidity of castor oil modified epoxy system (Ruseckaite et al, 1993) and those based on light scattering of epoxy/dicyandiamide /PES systems (Kim et al, 1993).

DGEBA/MTHPA /BDMA/PEK-C			DGEBA/MTHPA /BDMA/PES		
PEK-C/ [η] (dL/g)	*Ea(ps)*/kJ .mol^{-1}	R	PES [η] /(dL/g)	*Ea(ps)*/kJ .mol^{-1}	R
0.53	74.8	0.999	0.36	77.8	0.998
0.43	77.1	0.999	0.43	72.0	0.999
0.32	76.1	0.999	0.53	73.5	0.999

Table 7. E_a *(ps)* values for DGEBA/MTHPA /BDMA/TP systems with different TP molecular size, BDMA 0.9%

5.3 Effect of cure rate

In our research, initiator or catalyst was employed to accelerate the TS matrix cure rate, the more the initiator/catalyst content, the fast the cure reaction will be. It was observed that phase morphologies will change in size or patterns during the variation of cure rate, whereas the phase separation time-temperature dependences keep similar. Shown in Figure 10 are the linear correlations of $\ln t_{ps}$ vs. $1/T$ for DGEBA/MTHPA/BDMA/PEK-C system containing different level of initiator BDMA and AroCyL10/PEK-C system with different catalyst content of $Cu(AcAc)_2$. Since the initiator/catalyst contents are very limited, so the thermodynamics of the mixtures is supposed to approximately the same. According to the cure reaction mechanism, the higher the initiator or catalyst levels, the faster the consumption of the TS monomers, and the earlier the systems will be driven into the unstable region. Although the phase separation times are different for composites with different level of initiator/catalyst while the parallel layouts of curves in both of the two diagrams indicate the similar E_a *(ps)* values as summarized in Table 8, even though the morphologies change with variation of initiator levels (Cui et al, 1997; Montserrat et al, 1995).

The cure reaction activation energy E_a of systems with different level of initiator/catalyst was determined by Kisinger approach as shown in Table 8 as *Ea*. It was observed that when initiator content is ≥0.9%, cure reaction activation energy *Ea* values are similar in DGEBA/MTHPA/BDMA/PEK-C systems of different BDMA content. This is different from Montserat's finding (Montserat et al, 1995), which said that *Ea* generally decreased with increase of initiator level. It is presumably because the initiator content employed in our present systems is higher enough to catalyze the chain-wise copolymerization of DGEBA

and MTHPA during the temperature scan, and the higher *Ea* values in Montserat's systems probably arise from the uncatalyzed copolymerization for the deficiency of initiator BDMA. Similar results were observed in AroCyL10/Cu(AcAc)$_2$/PES systems.

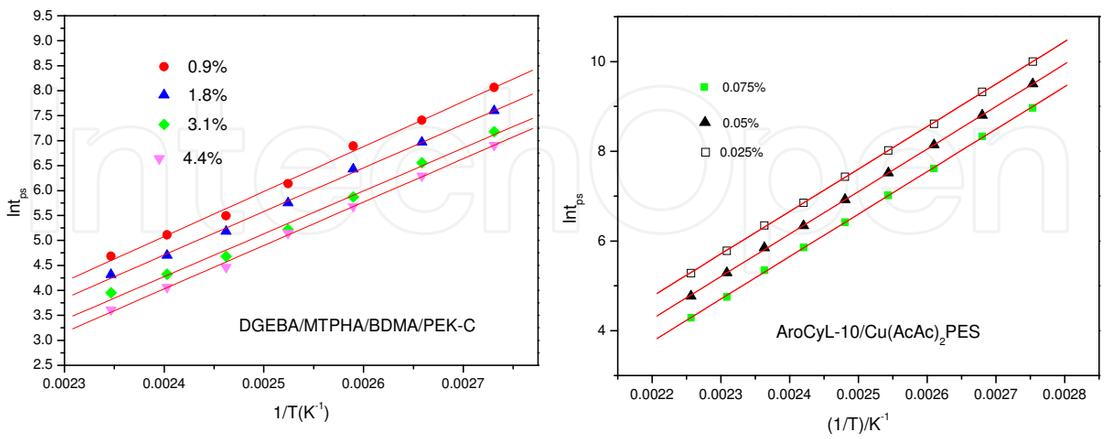

Fig. 10. lnt_{ps} *vs. 1/T* for DGEBA/MTHPA/BDMA/PEK-C10phr and AroCyL10/Cu(AcAc)$_2$/PES10phr with different initiator content (based on OM)

DGEBA/MTHPA/BDMA/PEK-C10phr					AroCyL10/Cu(AcAc)$_2$/PES10phr		
BDMA content/ wt.%	*Ea(ps)*/ kJ .mol^{-1}	R	*Ea*/ kJ .mol^{-1}	R	Cu(AcAc)$_2$ content/wt.%	*Ea(ps)*/ kJ .mol^{-1}	R
0.9	74.8	0.999	73.8	0.999	0.025	78.8	0.999
1.8	72.5	0.999	73.9	0.999	0.05	78.5	0.999
3.1	71.4	0.999	n.d.	n.d.	0.1	77.8	0.999
4.4	72.3	0.999	74.1	0.999	n.d.	n.d.	n.d.

Table 8. *Ea (ps)* for Epoxy/hardener/TP and Cyanate ester/TP systems with different initiator /catalyst content

5.4 Cure activation energy barrier and chemical environment effects on *Ea(ps)*

As depicted in Section 5.2 and 5.3 that *Ea(ps)* values are independent on the cure rate and also irrespective to the TP content and TP molecular size in the usual systems as far as TPs are used in minor part as toughening agents. But *Ea(ps)* varies with the cure activation energy barrier *Ea* and chemical environments, both of which will be discussed in the following subsections.

5.4.1 Cure path and cure activation energy effects on *Ea(ps)*

Shown in Figure 11 and Table 9 is the phase separation time/temperature relations in the range of 120-200℃ for systems of BMI/DBA/PEK-C10phr and BMI/DBA/PES 10phr respectively, together with the gel time/temperature data. It can be seen that the slope of Arrhenius plot of the phase separation and gelation in the 120-170℃ range is lower than that in the 180-200℃ range in both of the two systems. Correspondingly, the phase separation

activation energy E_a *(ps)* values in the range of 120-170 ℃ are lower than those in the range of 180-200℃. The change of temperature dependency on the phase separation times can be attributed to the complexity of the cure reaction between BMI and DBA. Although lots attempts have been made to elucidate the curing mechanism of BMI/DBA systems, these have been impeded by the complexities of the reaction multiple paths of the reaction. The following reaction types have been proposed to be involved in the curing process: ENE, Diels–Alder, homopolymerization, and alternating compolymerization. Allyl phenol compounds are expected to co-react with BMI to give linear chain extension by an ENE-type reaction in lower temperature range of 120-170℃ and show a lower cure activation energy barrier, and this is followed by a Diels–Alder reaction at a high temperature range of 180-200℃ with bigger cure activation energy (Mijovic & Andjelic,1996; Shibahara et al, 1998; Rozenberg et a,2001; Xiong et al, 2003).

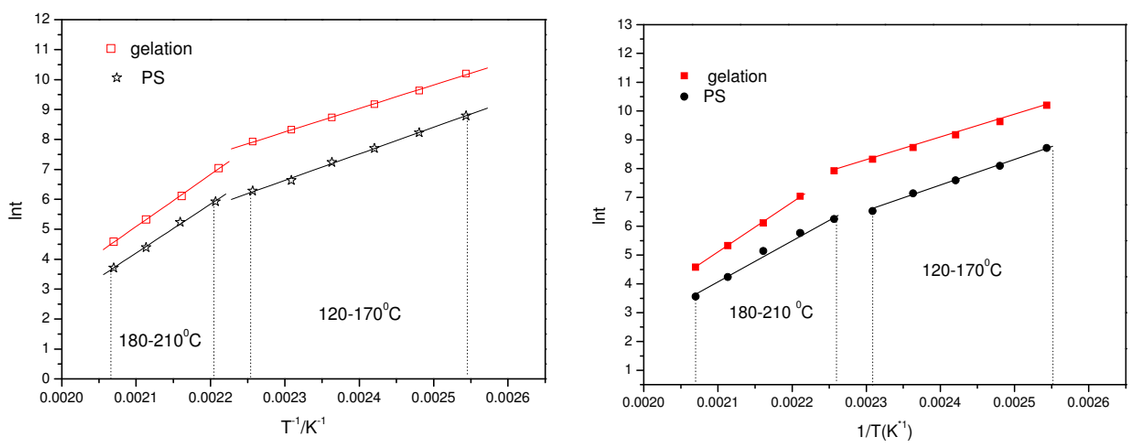

(a) (b)

Fig. 11. Phase separation time/temperature dependences in BMI/DBA/TP systems (by OM). (a) BMI/DBA/PEK-C. (b) BMI/DBA/PES

T/°C	BMI/DBA/PEK-C		BMI/DBA/PES		BMI/DBA	
	E_a*(ps)*/kJ .mol^{-1}	R	E_a(ps)/kJ .mol^{-1}	R	E_a*(gel)*/kJ .mol^{-1}	R
120~170	73.7	0.999	63.4	0.999	54.3	0.999
180~210	136.0	0.999	130.1	0.999	120.3	0.999

Table 9. Phase separation *Ea(ps)* values of BMI/DBA/TP 10phr systems

Systems	Initiation	*Ea(ps)*/ kJ .mol^{-1}	R	*Ea*/ kJ .mol^{-1}	R
DGEBA/MTHPA/PES10phr	Initiator 0.0%	83.9	0.999	75.5	0.999
	Initiator 0.9%	77.8	0.998	73.8	0.999
DGEBA/MTHPA/PEI10phr	Initiator 0.0%	82.3	0.999	88.3	0.999
	Initiator 0.9%	59.0	0.999	73.8	0.999

Table 10. *Ea(ps)* values for DGEBA/MTHPA/PES and DGEBA/MTHPA/PEI systems without and with BDMA

The effects of cure reaction energy *Ea(ps)* were also observed in DGEBA/MTHPA/PES and DGEBA/MHTPA/PEI systems as displayed in Table 10, wherein the initiator BDMA was employed or not. The reactions of DGEBA and MTHA with or without initiator BDMA are in different path. As reported that DGEBA and MTPHA reacts through the chain mode in the presence the catalyst such as tertiary amine BDMA with low activation energy compared to the stepwise polymerization of DGEBA and MTHPA (Fisch et al,1956; Fisch,1960). As shown in Table 10, both the DGEBA/MTHPA/PES and DGEBA/MTHPA/PEI systems without initiator BDMA show higher cure activation energy *Ea* values than the systems containing 0.9%BDMA, accordingly higher Ea(ps) values were observed. It should be pointed that in DGEBA/MTHPA/PEI system which shows UCST phase behavior, the *Ea(ps)* of composition without catalyst BDMA is much higher than the composition with BDMA. The cure activation energy changes in the range of $\triangle Ea$=14.5k J .mol^{-1}, while phase separation activation energy show the discrepancy of $\triangle Ea(ps)$=22.3k J.mol^{-1}, which is much higher than the former. It can be assumed that the significant increase of *Ea(ps)* of DGEBA/MTHPA/PEI composition is not only generated from the change of chemical reaction energy barrier *Ea*, while part of the increase of $\triangle Ea(ps)$ may come from the increase of the cure reaction temperature. In DGEBA/MTHPA/PEI composition, because the absence of initiator BDMA, the cure temperature has been elevated quite lot for cure efficiency, as was reported, DGEBA/PEI is a system of UCST phase diagram (Bonnaud et al, 2002), the elevation of cure temperature will increase the quench depth which possibly causes the increase of *Ea(ps)*. The physical scheme of the correlation and even similar value range implies the CIPS induced by the curing.

5.4.2 *Ea(ps)* dependence on stoichiometry in UCST TP/TS/hardener systems

Besides the chemical reaction energy barrier dependence of *Ea(ps),* it was observed that the *Ea(ps)* values also vary with the chemical environments, like stoichiometric balance, TP and TS monomer structures. We will discuss how the chemical environment factors will alter the phase separation activation energy in details. In this subsection, we only talk about the phase separation time-temperature dependence in TP modified TS systems with UCST type phase diagram, which can be explained quite well with the interaction energy density parameter in our research scope.

Shown in Figure 12 and Table 11 are the time-temperature dependence variation in DGEBA/DDM(DDS)/PEI10phr and DGEBA/MTHPA/BDMA/PEI10phr systems with different chemical stoichiometric ratio *r*. As can be seen in DGEBA/DDM/PEI system which shows UCST type phase behavior (Bonnaud et al, 2002), the phase separation activation energy values *Ea(ps)* of it increase with *r*, when *r*=1.5 the system even shows no phase separation. While in DGEBA/DDS/PEI system, *Ea(ps)* changes with *r* in an opposite way. In view of chemical reaction energy barrier, E_a does not change with the stoichiometric ratio *r* for both of the DGEBA/DDM/PEI and DGEBA/DDS/PEI systems as displayed in Table 11 by value of *Ea*. The changes of *Ea(ps)* possibly originate from the variation of chemical environments with the change of stoichiometric ratio, e.g. the miscibility between components is altered with the increase of *r* values, which in turn influence the *Ea(ps)* substantially. We calculated the interaction energy density *B* values for different combination as shown in Table 12. It can be seen that the miscibility of PEI with DDS is worse than that it with the cured DGEBA/DDS. So it can be hypothesized that the more of

DDS, the poorer the miscibility between TP and cured TS and the easier for the onset of phase separation with lower *Ea(ps)*. The inverse scenarios were observed in DGEBA/DDM/PEI systems, wherein DDM is unfavorable for demixing of the components of TP and TS, DDM shows better affinity to PEI than the cured DGEBA/DDM matrix, so the more the DDM content, the better the compatibility between the components and the bigger *Ea(ps)* value it exhibits. Similar phenomena were observed in DGEBA/MTHPA/PEI systems which can also be explained in the frame of interaction energy density parameter.

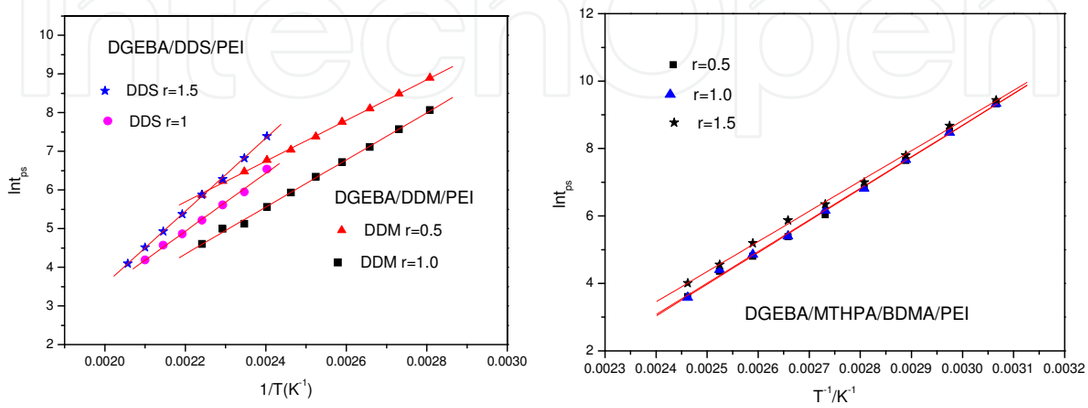

Fig. 12. Plots of $\ln t_{ps}$ vs. *1/T* for TP/ TS/hardener systems with different stoichiometry *r* values

	DGEBA/DDM/PEI		DGEBA/DDS/PEI		DGEBA/MTHPA/BDMA/PEI	
r	*Ea(ps)*/ kJ .mol^{-1}	*Ea(gel)*/ kJ .mol^{-1}	*Ea(ps)*/ kJ .mol^{-1}	*Ea(gel)*/ kJ .mol^{-1}	*Ea(ps)*/ kJ .mol^{-1}	*Ea(gel)*/ kJ .mol^{-1}
0.5	43.8	46.3	no demixing	61.1	56.3	51.2
1.0	50.6	44.6	78.6	58.1	56.2	51.6
1.5	No ps	44.7	62.2	59.7	59.70	51.7

Table 11. Values of *Ea (ps)* for different TP/TS/hardener systems with different stoichiometric ratios *r*

B/J.cm^{-3}	DGEBA/DDM	DGEBA/DDS	DGEBA/MTHPA	DDM	MTHPA	DDS	AroCyL-10
PEI	5.61	0.12	6.80	3.60	0.50	2.48	3.17
PEI_1	3.13	0.89	4.03	1.68	0.012	4.72	5.67

Table 12. Interaction energy density *B* values between different combinations

5.4.3 TP and TS structure effects on *Ea(ps)* in UCST type TP/TS/hardener systems

Besides the chemical stoichiometric balance, TP or TS structure variation all take substantial effects on the phase separation time-temperature dependence. As shown in Table 13, the phase separation activation energy *Ea(ps)* varies seriously with the poly(ether imide) structures changing, either in epoxy/amine and epoxy/anhydride matrices, or in cyanate ester systems. PEI and PEI_1 have different chemical structures as shown in Table 1, both of them show different miscibility with matrices of DGEBA/DDM and DGEBA/DDS respectively. In DGEBA/DDM matrix, PEI_1 show higher affinity to the matrix than PEI does,

so it can be understood that even no phase separation was observed in DGEBA/DDM/ PEI_1 for the excellent compatibility; while in DGEBA/DDS matrix, miscibility trend reverses, PEI is more favorable to phase mixing than PEI_1 as denoted by the higher *Ea(ps)* value of 78.6 k J .mol^{-1}. Similar phenomena were observed in the matrix of DGEBA/anhydride/PEI and AroCyL10/PEI respectively. In AroCyL10/Cu(AcAc)2/PEI1 system PEI1 even can't be dissolved in the matrix homogenously within the experimental condition for the poor miscibility of the TP and AroCyL10 monomers, the bigger interaction energy density parameter *B* in Table 15 gives the reasonable interpretation. In all these mixtures, the variations of *Ea(ps)* because of PEI structure dissimilarity can be well interpreted by the interaction energy density theory.

TP	Ea(ps) /kJ .mol-1	R	Ea(gel)/ kJ .mol-1	R	Ea(ps) /kJ .mol-1	R	Ea(gel) /kJ .mol-1	R
	DGEBA/DDM matrix				DGEBA/DDS matrix			
PEI1	no ps	-	51.6	0.999	61.2	0.999	62.8	0.999
PEI	50.6	0.999	51.0	0.999	78.6	0.999	62.5	0.999
TP	DGEBA/MTHPA matrix				AroCyL10/Cu(AcAc)2 matrix			
PEI1	72.6	0.999	52.7	0.999	Immiscible	/	60.9	0.999
PEI	59.7	0.999	51.6	0.999	47.9	0.999	61.2	0.999

Table 13. Phase separation time-temperature dependence of TS/hardener/PEI systems with different TP structure

Epoxy monomers	Ea(ps)/kJ.mol^{-1}	R	Ea/kJ.mol^{-1}	R
E56	54.7	0.999	51.4	0.999
E54	52.6	0.999	/	/
E51	52.4	0.999	51.6	0.999
E44	44.3	0.999	/	/
E39	40.3	0.999	51.2	0.99
E51/ E44(1:1,ratio by weight)	48.7	0.999	/	/
E51/E39 (1:1,ratio by weight)	40.1	0.999	/	/
E51/ E31(4:1,ratio by weight)	36.2	0.999	52.1	0.999

Table 14. *Ea (ps)* for epoxy/DDM/ PEI systems with different epoxy monomer structures

The phase separation time-temperature dependencies also changed with the variation of TS monomer structures, as shown in Table 14, with the increase of epoxy molecular weight, *Ea(ps)* changes substantially. Here all the epoxy monomers have the structures referring to Table 1, only differing in the number of repeating unit n, the numbers beside "E" in Table 14 donating the epoxide value of the epoxy monomer, like E54 means monomer contains 0.54mol epoxide functional group per 100g DGEBA., The smaller epoxide value, the bigger the monomer size. As can be seen that the phase separation activation energy Ea(ps) decreases with the increase of molecular size of epoxy monomer DGEBA. Interaction energy density parameter *B* values between the cured DGEBA/DDM matrix and PEI were

calculated and summarized in Table 15. As was shown that the growth of DGEBA monomer size give higher *B* value implying the widening of miscibility mismatch between TP and TS components. This is apparently contradictory to the finding in above section wherein TP content and size show limited effect on *Ea(ps)* values. It is true that the increase of DGEBA molecular size will change the phase diagram location as were observed, but except the DGEBA size effect on phase behavior, there is another favoring factor for phase separation is the volume fraction change of cure agent DDM because of the increase of DGEBA size. Bigger DGEBA gives higher molar volume fraction which means small volume fraction remained for cure agent DDM. DDM is a component which is very favorable of phase mixing, the less of DDM volume is, the worse the miscibility of TP and TS will be.

B(J.cm^{-3})	E56/DDM	E54/DDM	E51/DDM	E44/DDM	E39/DDM	E31/DDM
PEI	5.53	5.56	5.61	5.74	5.83	10.71

Table 15. Change of interaction energy density parameter *B* for the variation of epoxy monomer structures

5.4.4 Stoichiometry and TP and TS structure effects on *Ea(ps)* in LCST type TP/TS/hardener systems

The interaction energy density theory works well in rationalization of the phase separation time-temperature dependence on the chemical environment change: ether coming from stoichiometric imbalance, or TP and TS structures in the TP/TS systems with UCST phase behavior. But such theory is not universal in TP/TS systems with LCST phase diagrams.

Shown in Table 16 are the phase separation activation energy *Ea(ps)* values of DGEBA/DDM/PES (Bonnaud et al, 2002) and DGEBA/MTHPA/PES with different stoichiometry *r* both of which show LCST type phase diagram. As was shown that both of *Ea(ps)* values increase with the descending of *r* value. The interaction energy density parameter *B* of PES/harder and PES/(cured TS) are calculated and displayed in Table 18. It was found that both of the two hardeners of DDM and MTHPA show higher affinity to PES than the corresponding cured resin, while the experimental observations did not support the theoretical prediction, the higher the hardener content was, the smaller the phase separation energy barrier appeared. The apparent paradoxical phenomenon comes from the limitation of the present thermodynamics in depicting polymer mixture phase separation process, which will be explained in following content within this section.

	DGEBA/DDM/PES				DGEBA/MTHPA/PES			
r	Ea(ps) /kJ.mol^{-1}	R	Ea(gel) /kJ.mol^{-1}	R	Ea(ps) /kJ.mol^{-1}	R	Ea(gel) /kJ.mol^{-1}	R
1.5	53.7	0.999	44.7	0.999	72.8	0.999	70.2	0.999
1.0	58.6	0.998	44.6	0.998	77.8	0.999	70.3	0.999
0.5	62.4	0.998	46.3	0.998	78.3	0.999	70.7	0.999

Table 16. *Ea(ps)* variations in DGEBA/DDM/PES and DGEBA/MTHPA/PES systems with different *r*

Besides the stoichiometric effects on the variation of phase separation activation energy *Ea(ps)* in various TP modified TS systems which show LCST phase diagrams, the chemical environments effects arising from TP and TS structure alterations were also studied. Here we mainly talk about some representative systems, like DGEBA/DDM/TP, DGEBA/MTHPA/BDAM /TP and Cyanate ester system of AroCyL10/TP (Hwang et al, 1999) as in Table 17, wherein TP structure varies in repeating units.

Based on interaction energy density parameter calculation between different combinations as shown in Table 18, it can be seen that in DGEBA/DDM/TP systems, PEK-S shows highest affinity to the matrix, then PSF and PES show dropping affinity to matrix in sequential. While the measured *Ea(ps)* values have not shown the corresponding theoretical sequence. It can be seen that DGEBA/DDM/PES-C with highest miscibility did show biggest phase separation energy barrier, e.g. no phase separation was observed upon completion of the cure. But DGEBA/DDM/PES shows a higher *Ea(ps)* value than that of DGEBA/DDM/PSF system which is contrary to theoretical prediction. Inconsistence was also observed in other systems, e.g. DGEBA/MTHPA/PEK-C systems, *Ea(ps)* doesn't show a monotonic relationship with the calculated *B* value.

All these experimental and theoretical discrepancies arise from the limitation of the present cohesive energy theory of interaction energy interaction density. Indeed, volume fraction change during cure, strong hydrogen bonding and strong polar interaction are not included in our calculation. These effects could be critical for the phase behavior, especially in the LCST systems, so further theoretical and experimental efforts are to be made. Up to now, all the theoretical analysis works only well in UCST systems where hydrogen bonding and other special energy effect are absence. But for the LCST systems, as have been found in this subsection, most of the experimental results contradict the theoretical hypothesis.

TP type	DGEBA /DDM/TP		DGEBA /MTHPA/TP		AroCyL-10/TP	
	Ea(ps) /kJ.mol^{-1}	Ea /kJ.mol^{-1}	Ea(ps)/kJ.mol^{-1}	Ea /kJ.mol^{-1}	Ea /kJ.mol^{-1}	Ea(ps) /kJ.mol^{-1}
PES	60.1	50.7	60.1		78.5	60.8
PSF	55.9	51.6	55.9		70.3	65.2
PES-C	No PS	51.9	No PS		/	/

Table 17. *Ea(ps)* variation for the change of TP structure in matrix of TS/hardener/TP mixtures

B(J.cm^{-3})	DGEBA/DDM	DDM	DGEBA/MTHPA	MTHPA	AroCyL-10
PES	16.56	12.68	19.00	9.38	31.2
PSF	6.60	/	7.02	/	47.6
PES-C	3.13	/	3.42	/	/

Table 18. Calculated *B* for PES, PSF and PES-C with TS components

5.4 Time-temperature transformation diagram with phase separation

As was known that all the processing of thermosetting composites are carried out in wide time/temperature space as presented by TTT (time–temperature-transformation) diagram (Enns & Gillham,1983;Gillham,1986). Phase separation usually occurs before the chemical

gelation, which is always accompanied by the change of viscosity or modulus as shown by Figure 2 in Section 3. Following phase separation is the chemical gelation of TS rich phase, which retards the resin flow and limits the coarsening of the dispersed phase domain. Upon vitrification, curing ceased totally because the freezing of the component chain.

For TP modified TS processing, the cure time-temperature routine has a great impact on the morphology generated during cure further to the final material properties (Inoue, 1995; Williarms, 1997). To get TP/TS material with desired structure and properties, it is necessary to design the cure time-temperature processing routine. The time-temperature dependence of gel and vitrification is well illustrated by the kinetic approach for the systems with unambiguous cure kinetics (Wisanrakkit & Gillham,1990). It is desired to have the phase separation zone defined in the TTT diagram for TP/TS composite processing. So far only schematic diagram appeared in literatures (Williams, et al. 1997). This situation is obviously related to the issue of determination of phase separation time in broad temperature range.

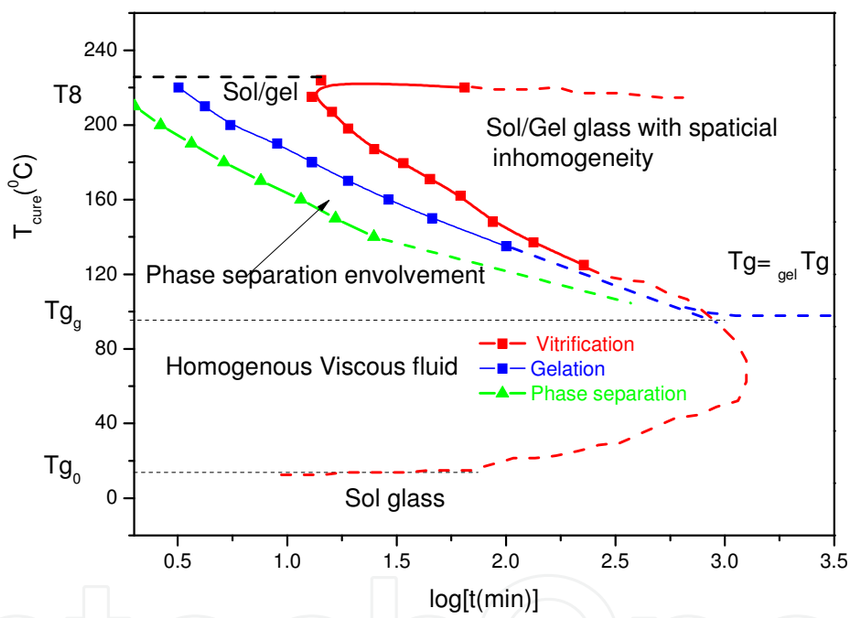

Fig. 13. TTT diagram depicting occurring times for phase separation, chemical gelation and vitrification for Epoxy/DDS/ PEK-C 15phr system

Based on our efforts on the phase-separation time-temperature dependence relationship and the TS matrix cure kinetics, it is now convenient to build the Time-Temperature Transformation Diagram (TTT) accompanied with phase separation process (TTT-PS diagram). Figure 13 displays the example of experimental determined TTT-PS diagram, which defines the main events taking place during the curing of TP modified TS with the presence of CIPS in whole time-temperature window. Obviously the TTT-PS diagram may be of great importance for composites processing where morphology and structure control is of interests. It is shown in Figure 13 that in the measured Epoxy/DDS/PKE-C system with a LCST phase behavior, the phase separations take place before chemical gelation throughout the cure temperature range employed, and the phase separated structure was

even observed at temperature where the epoxy matrix started degrading with volatiles coming out. In some TP/TS mixture, e.g. UCST systems, phase separations could only take place in certain time-temperature space within the up-merging curves of phase separation and gelation. Even in this area PS is not guarantied, because of the PS dynamics at early critical stages and the pattern developing dynamics. In Figure 13, the phase separation and gelation time-temperature curves in the semi-log coordinator at low temperature range are extrapolated in a convergent direction intentionally to depict to what will happen at low temperature. It can be assumed theoretically that the phase separation time-temperature curve and the gelation time-temperature will converge below certain temperature. This is because our present mixture shows LUST phase behavior. The decrease of temperature is favorable of phase mixing which possibly will contribute to a higher phase separation activation energy; on the other hand, the cure reaction will become difficult because the restrain on component mobility generated by the high viscosity accompanying the temperature decrease.

6. Morphology evolvement in PS and dynamic theory prediction

6.1 Dynamic theory for morphology evolvement

The thermodynamic theory reveals the possibility of phase separation (PS), the phase separation possible mechanism like spinodal & bimodal decompositions, and the conditions of PS emerging, while it does not answer how the PS pattern develops, e.g. the phase separation dynamics. To understand the phase pattern evolvement (for example in Figure 7) and control the morphology in processed product, the phase separation dynamics has been intensively studied in the past three decades from both experimental and theoretical viewpoints(Onuki,1986; Onuki & Taniguchi 1991; Tanaka, 1997; Onuki & Taniguchi 1997). Experimental observations of CIPS disclosed spectacular variable schemes of morphology changes depending on the composition and process parameters. Good news is that owing to the advances of condensed matter physics a unified scheme became possible to explain the complex phenomena. From the concept of dynamic universality of critical phenomena, phase separation phenomena have been classified into various theoretical models. For example, phase separation in solids is known as the "Solid Model or Model B" (Hohenberg & Halperin, 1977), where the local concentration can be changed only by material diffusion, while phase separation in fluids is known as the "fluid model or model H" by both diffusion and flow (Doi&Onuki, 1992). It has been established that within each group the behavior is universal and does not depend on the details of the material. The classic theories consider the same dynamics for the two components of a binary mixture, which we call "dynamic symmetry". However, such an assumption of dynamic symmetry is hardly valid in ''complex fluids''. For the example of TP/TS mixtures, their molecular mass, diffusivity and mobility are very different. For these ''dynamic asymmetric'' systems one needs to consider the interplay between critical dynamics and the slow dynamics of polymer itself which was in so called ''Viscoelastic Model'' (Tanaka, 1997).

Some researches have been focused on the CIPS process starting from homogenous solution using Onuki's Elastic solid model (Zhang, 1999) or "two fluid" model or Tanaka's viscoelastic model (Tanaka, 1997). Which model should one choose depends what dominant physical parameters are involved in the system. For example, at the early stage of spinodal

phase separation of high viscous mixture, diffusion is dominant, so elastic solid model may work well enough, while in late stage under interfacial tension at gradually clearer phase border the drop merging becomes important and solid model may underestimate the pattern coarsening. Simulation is often a necessary approach to "image" the events take place in the black box where we can't tough directly by any means for its complexity, while numerical solutions work successfully.

In our present work, the modified Elastic Model of Onuki (Onuki & Taniguchi 1991) was employed, the phase separation dynamical equation was numerically solved, using the so-called cell dynamical system presented by Oono and Puri (Oono & Puri 1988).

The free energy functional of the system F is given by (Onuki, 1997; Zhang, 1999):

$$F = \int d\mathbf{r}[f(\phi) + \frac{1}{2}|\nabla\phi|^2 + a\phi\nabla \bullet \mathbf{u} + \frac{1}{2}K|\nabla \bullet \mathbf{u}|^2 + \mu Q] \tag{12}$$

Wherein $f(\phi) + 1/2|\nabla\phi|^2$ is the free energy of unit volume in the Flory-Huggins average lattice theory or Ginzberg-Landau theory, a is a parameter represents the coupling constant of concentration gradient and elastic field, u is the deformation vector. In linear viscoelastic region, the bulk elastic energy originates from the bulk modulus K and symmetric conformation tensor Q, which are irrespective to volume fraction Φ, and shear energy comes from the shear modulus μ and symmetric conformation tensor Q:

$$Q = \frac{1}{4}\sum_{i,j}[\nabla_i u_j + \nabla_j u_i - \delta_{ij}\frac{2}{d}\nabla \bullet \mathbf{u}]^2 \ , \ \nabla_i = \frac{\partial}{\partial x_i} \tag{13}$$

Wherein d is the spatial dimension μ and concentration ϕ is supposed to be linear as:

$$\mu = \mu_0 + \mu_1\phi \tag{14}$$

Based on the force equilibrium requirement of $\frac{\delta F}{\delta u_i} = 0$ we can use the following equation to replace u in equation 12, at the same time we can get the relationship of concentration and elastic energy:

$$\delta u_i = -(\alpha / K_L)\frac{\partial\omega}{\partial x_i} \tag{15}$$

$$\nabla^2\omega = \phi - \bar{\phi} \tag{16}$$

Where $\bar{\phi}$ is the spatial average concentration, K_L can be correlated to bulk modulus through equation 17：

$$K_L = K + 2(1 - 1/d)u_0 \tag{17}$$

Under infinitesimal deformation near equilibrium, the symmetric conformation tensor Q can be extended based on δu ，and only first order approximation is left.

$$\hat{Q} = (\alpha / K_L)^2 \sum_{i,j} [\nabla_i \nabla_j \omega - \frac{1}{d} \delta_{ij} \nabla^2 \omega]^2 \tag{18}$$

For simplicity, all the constant part in the free energy, the free energy functional can be expressed as

$$F = \int d\mathbf{r} [f(\phi) + \frac{1}{2} |\nabla \phi|^2 + \mu_1 \phi \hat{Q}] \tag{19}$$

And with equation 18, we can construct the TDGL（time dependent Ginzberg Landau）equation：

$$\begin{aligned} \frac{\partial \phi}{\partial t} &= M \nabla^2 \frac{\delta F}{\delta \phi} = M \nabla^2 [\frac{\partial f}{\partial \phi} - \kappa \nabla^2 \omega \\ &+ G_E \hat{Q}] + 2G_E \sum_{i,j} \nabla_i \nabla_j \phi [\sum_{i,j} \nabla_i \nabla_j \phi - \frac{1}{2} \delta_{ij} (\phi - \bar{\phi})] \end{aligned} \tag{20}$$

Where in

$$g_E = \mu_1 (\alpha / K_L)^2 \tag{20a}$$

is the modulus of TS phase, it changes with the cure time for the increase of TS size, for most of the TS monomers reaction through the second order reaction. According to the chemorheology of curing, one can get the time-temperature dependence of dynamic viscosity change. Therefore, in our simulation, we use the expression g_E～(TS conversion)

$$1 / ((1 - \exp(-\mathrm{Ea} / \mathrm{RT}) * \mathrm{t}) \tag{20b}$$

The Ginzberg-Landau free energy is simplified as following:

$$\frac{\partial f}{\partial \phi} - \kappa \nabla^2 \phi = -\phi + \phi^3 - \nabla^2 \phi \tag{21}$$

By numerical calculation of governing equation of 16, 20 and 21 we can get the qualitative information about what happened in the intermediate and later stager of CIPS using the modified "Solid Elastic Model" wherein modulus mismatch between TP and TS varied along time. Shown in Figure 14 is a simulation result for the systems with "Viscoelastic symmetric" modulus. The volume fractions of TP component is φ=0.5. As can be seen in the "dynamic viscelastic symmetric" system, bi-continuous phase was observed at early stage and some coarsening of the networks appear with time until at last TP network morphologies freeze , because of full gelation of TS phase

In some TP/TS/Hardener systems when the TP molecular is not high enough or TS monomers show high hydrodynamic effect upon phase separation, second phase separations were always observed. By the present "Elastic Solid Model", such scenario can't be incorporated, wherein in the ''Two Fluid Model'' coupled with chemical reaction works

better. But for the composites material fabrication, the final morphology though too much interface sharpening and phase coarsening via flow may not a favorite process.

In the real processing of composites material during fabrication of large parts, like composite aircraft wind and fuselage, incomplete diffusion with elastic misfit between the components does exist, wherein the TP and TS are interlaminated during RTM (resin transfer molding). Based on ex situ toughening concept, the thin TP layers are periodically interleaved the TS/graphite prepreg plies, the respective TP and TS components were separated. After the wet prepregs are laminated, the interaction between TP and TS phase and the diffusion couples with the cure reaction and phase separation start (Yi,2006;Yi et al, 2008; Yi & An,2008; Yi, 2009). In such delicate, hard to monitor process, the computer simulation can play role. We will discuss such simulation process with modified Onuki "Elastic Solid Model" in subsequent section.

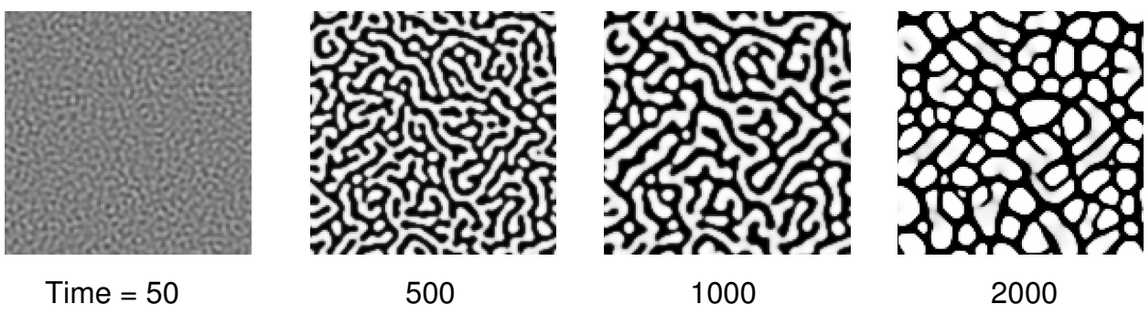

Fig. 14. Morphology evolvement of two components mixture with symmetric moduli. t donating the dimensionless time in the temporal space. Volume fraction is 50%

6.2 Spatially inhomogeneous structure with concentration gradient

In Section 6.1 we simulate what happens in the *in situ* phase separation process, wherein the phase separated structures are distributed spatially evenly in the matrix, phase inversion mechanism was clearly displayed. Here, we will use the same phase separation thermodynamic and similar kinetic frame to monitor the events happened in *ex situ* toughening process, where interleaved TP and TS layered are layout periodically in spatial direction. By a similar two dimension CDS process , a linear concentration gradient is assumed along y-coordinate, our computational space is graded in square of size 0<x<L and 0<y<L, wherein L is the dimensionless square grid length, the concentration gradient is shown as $\phi(y) = \frac{1}{L} * y$ and $\frac{d\phi}{dx} = 0$, where in ϕ is the volume fraction of minor component TP.

Other thermodynamics and phase separation dynamics descriptions keep the same as Section 6.1 wherein in situ phase separation process is calculated by the CDS approach. In the present system, Shown in Figure 15 are simulated morphology evolving process with varying TP and TS modulus mismatch value of *Ge*. It can be observed that the higher the asymmetry is, the more inverted structures formed in the interface between TP and TS matrices. In a *Ge*=100 system, bi-continuous and inversion structures appear throughout the direction perpendicular to the layer plane, and also the morphology distribution varies along the same direction.

Shown in Figure 16 is the experimental SEM (Scanning Electronic Microscope) observation on the fractured interface between the epoxy BEP/DDS matrix and thermoplastic PEK-C layer. The morphology size and pattern vary periodically in direction perpendicular to ply direction. The simulation scenarios fit the experimental results qualitatively. In the future, improvements of present model with incorporation of spatial temperature ingredient and cure cycle possibly will give more clues to how the morphologies evolve during the real composite manufacture process.

IntechOpen

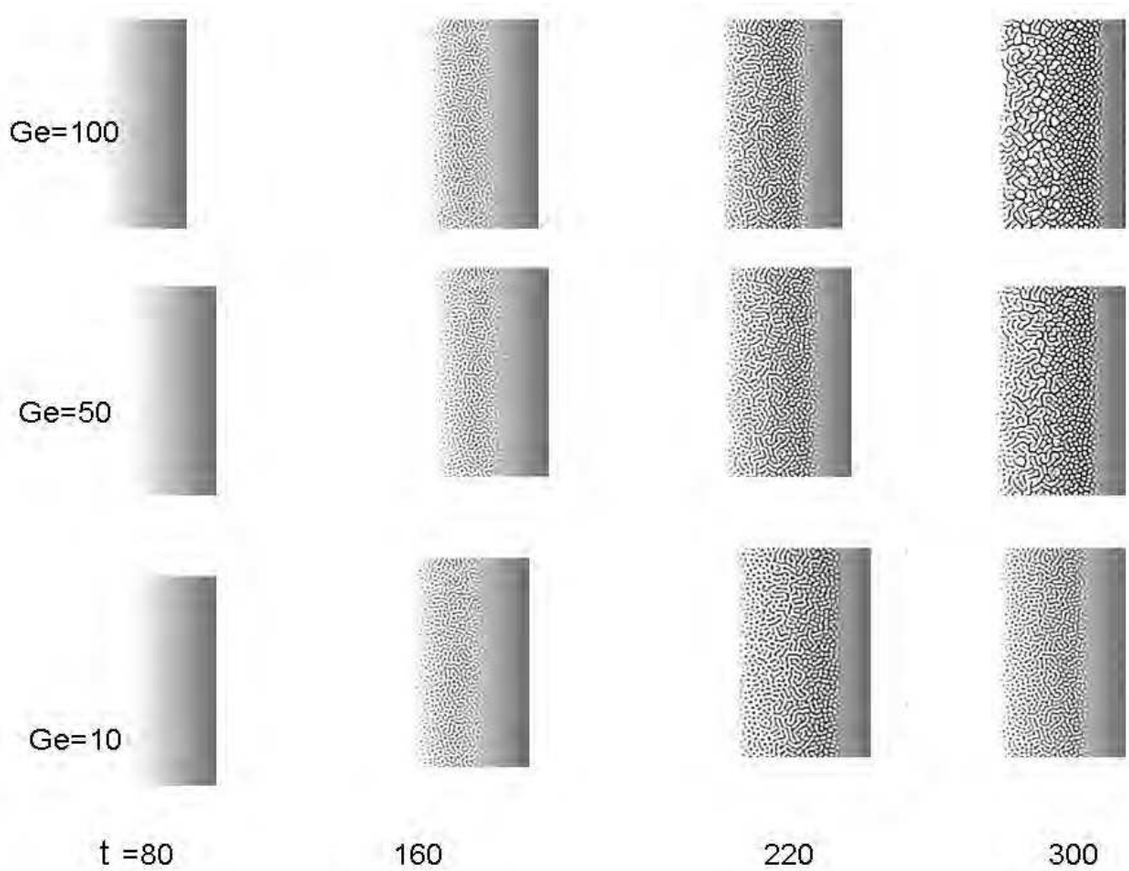

Fig. 15. Effect of modulus mismatch value Ge on the morphology distribution in direction perpendicular to ply

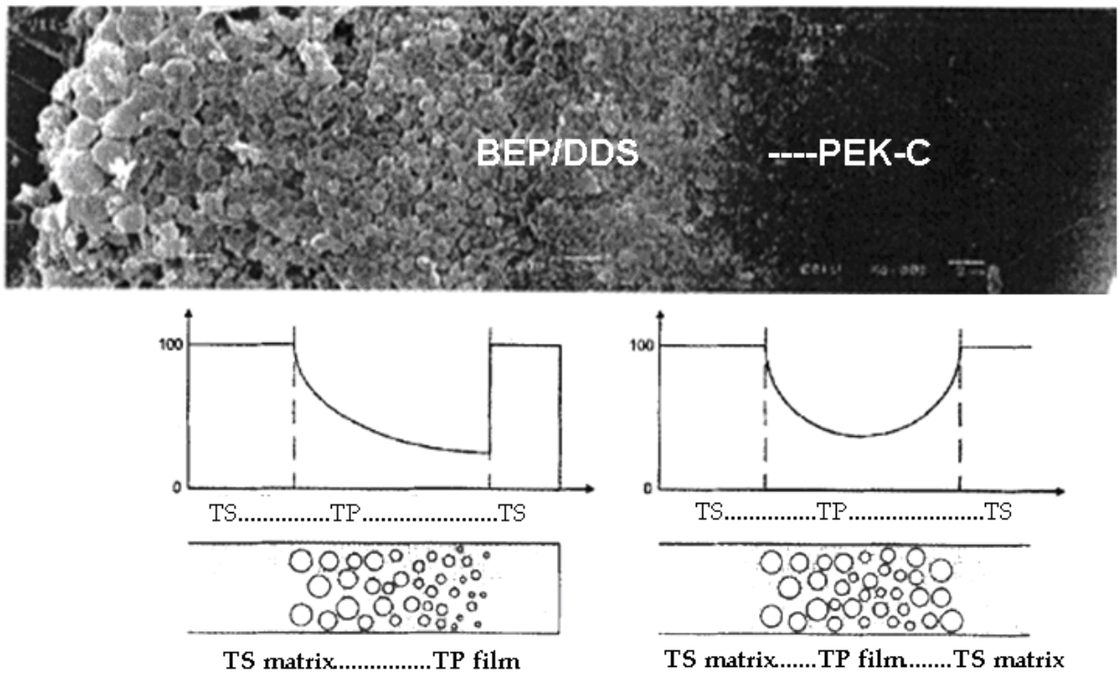

Fig. 16. Morphology distribution of an etched TP/TS/graphite composite toughened by ex-situ interlaminar process, observed by scanning electron microscope

7. Concluding remarks

In the past three decades, numerous experimental and theoretical achievements dealing with reaction-induced phase separation (RIPS) of polymer systems were driven by versatile applications in spite of the complex nature of the subject from the theoretical point of view. Cure induced phase separation (CIPS) is an important part of RIPS due to its innovative applications to composite processing, or more generally, to the innovations of multi-phase polymers. Instead of fight with interfacial tension in polyblends, CIPS processes involve the creation of phases with granular or network morphologies, the interfacial sharpening & coarsening according to the balance of diffusion and convection of viscous mobile systems, the termination of PS or the secondary PS affected by TS gelation and vitrification. It seems to be a disadvantage to allow the morphology influenced by so many factors, but it's also an advantage to have many means to create the structure we want, if we know the control rules. The intention of this review was using our practice to provide a qualitative (or partially quantitative) basis for readers to rationalize the numerous factors in CIPS process to achieve the desired morphologies and composite properties.

In the first section it was shown that: a) the purpose of modifying a high performance TS polymer composite is calling on innovative multi-scale matrix design; b) to achieve high toughness and, at the same time, high rigidity, the controllable micro-inhomogeneity including bi-continuous network with adjustable interface could be a good option for composite matrices; c) cure induced phase separation of the mixture of thermosetting resin (TS) with engineering plastics (TP) provide promising approach to do so. d) a gradient design of PS fitted in layered composite can even more optimize its performance.

To detect and study CIPS process comprehensively, one need multi measuring means, including necessary experimental innovations, which are summarized as: a) to detect the phase separation time (PS) in early stage, a patented transmission optical morphology analyzer (TOM) allows determining PS time and tracing the image evolvement of micro-phase separation at high T and long time; b) comparative studies using OM, SALS & dynamic rheology found two critical transitions: TP gelation by PS and a TS gelation, revealed the loose fractal network structure of TP at PS and TS fractal network at "critical gel states" and determined the network fractal dimensions.

Based on these "on-line" experimental approaches we were able to study the cure reaction of TP/TS with PS in broad time-temperature range. The temperature dependence of PS time was found experimentally to obey Arrhenius type rule for various TP/TS/hardener systems and PS activation energy may be defined and its relations to many compositional parameters were clarified experimentally. We were able to build the Time-Temperature-Transformation diagram including phase separation (TTT-PS) experimentally, which is of essential importance for TP/TS composite processing. There is still long way to go to answer the following questions thoroughly: why the CIPS happens? What governs the phase separated morphology development? How to predict the appearing of CIPS from the chemical formulation and processing parameters? However, some progresses in this direction can build a promising picture: a) like all mixing thermodynamics, Flory-Huggins mean field theory can be performed for CIPS. Instead using interaction parameter χ, the interaction energy density B was employed with more reasonable physical meaning and good relation with cohesive energy and, thus, chemical structures of the components; b) for the dynamically very asymmetric system, the viscoelastic phase separation theory by incorporating the reaction kinetics into time dependent Ginsburg-Landau (TDGL) equation and cellular-automata simulation can simulate the morphology development. If interlaminate diffusion is cooperated, the gradient morphology in layered composite can be simulated; c) our practice and the theoretical background are well situated in a multi-physics frame. Either thermodynamic or dynamic theory is all in mesoscopic level, with unified rules and leaving lower level chemical reactions and structures in parameters. This paradigm should work and be proved further in our efforts to build better composites.

Most of our researches were carried out under the support of National Key Basic Research Program (973 Program, 2003CB615600)

8. Reference

An, X.F. Study on Laminated-Toughened CFRPs Based Thermoset/Thermoplastic Diphase System. PhD Dissertation, (2004), Zhejiang University

Bicerano, J. (2002-08-01).*Prediction of Polymer Properties*, (3rd Edition), CRC Press, ISBN: 0824708210

Bonnaud, L.;Pascault, P. J. ; Sautereau, H. Kinetic of a Thermoplastic-Modified Epoxy-Aromatic Diamine Formulation: Modeling And Influence of a Trifunctional Epoxy Prepolymer. (2000). *Eur. Polym. J.*,Vol. 36, No.7, pp.1313-1321

Bonnet, A.; Pascault, J.P.; Sautereau, H.; Camberlin, Y. Epoxy-diamine Thermoset/Thermoplastic Blends. 2. Rheological Behavior Before and after Phase Separation. (1999). *Macromolecules*, Vol.32, No.25, pp.8524-8530

Bonnaud, L.; Bonnet, A.; Pascault, P. J.; Sautereau, H.; Riccardi, C. C. Different Parameters Controlling the Initial Solubility of Two Thermoplastics In Epoxy Reactive Solvents. (2002). *J. Appl. Polym. Sci.*, Vol. 83, No. 6, pp.1385–1396

Borrajo, J.; Reccardi, C.C.; Williams, J.J.R. Rubber-Modified Cyanate: Thermodynamic Analysis Of Phase Separation. (1995). *Polymer*, Vol.36, No.18, 3541-3547

Bucknall, C B, Gomez, C M, Quintard, I. Phase-Separation from Solutions of Poly(Ether Sulfone) in Epoxy-Resins. (1994). *Polymer*, Vol.35, No.2, pp353-359

Bucknall, C.B.; Gilbert, A. H. Toughening Tetrafunctional Epoxy Resins Using Polyetherimide. (1989). *Polymer*, Vol. 30, No.2, pp.213-217

Bucknall, C. B.; Partridge, I. K. Phase Separation In Epoxy Resins Containing Polyethersulphone. (1983). *Polymer*, 24, pp.639-644

Cadenato, A.; Salla, M. J.; Ramis, X.; Morancho, M. J.; Marroyo, M. L.; Martin, L. J. Determination of Gel and Vitrification times of Thermoset Curing Process by Means of TMA, DMTA and DSC Techniques TTT Diagram.(1997). *J. Therm. Anal.*, Vol. 49, 269-279

Chambon, F.; Petrovic, S.Z.; Macknight, J.W.; Winter, H.H. Rheology of Model Polyurethanes at the Gel Point.(1986). *Macromolecules*, Vol.19, No.8, pp.2146-2149

Chen,C.M; Hourston, J.D.; Sun,B.W. the Morphology and Fracture Behaviour of a Miscible Epoxy Resin-Polyetherimide Blend. (1995). *Eur.Polym.J.* Vol.31,No.2,pp199-201

Cheng, Q.F.;Fang, Z.P.;Xu, Y.H.;Yi, X.S. Morphological and Spatial Effects on Toughness and Impact Damage Resistance of PAKE-toughened BMI and graphites. (2009). *Chinese Journal of Aeronautic*, Vol.22，pp87-96

Cho, B.J J. ;. Hwang, W.; Cho, K. ; An, H. J. Park, E.C. Effects of morphology on toughening of tetrafunctional epoxy resins with poly(ether imide). (1993). *Polymer,* Volum.34, No.23, pp.4832-4836

Cui, J.; Chen, W.J.;Zhang, Z.C.; Li, S.J. Studies on the Phase Separation of Polyetherimide-Modified Epoxy Resin 1.Effect of Curing Rate on the Phase Structure. (1997). *Macromol. Chem. Phys.*, Vol.198, No6, pp.1865-1872

Doi,M; Onuki,A. Dynamic Coupling Between Stress And Composition In Polymer Solutions And Blends.(1992). *J. Phys. II France 2*, pp.1631-1656

Eloundou, P.J.; Gerard, F.J.; Harran, D.; Pascault, P.J. Temperature Dependence of the Behavior of a Reactive Epoxy- Amine System by Means of Dynamic Rheology. 2.High-Tg Epoxy-Amine System.(1996). *Macromolecules,* Vol.29, No.21, pp.6917-6927

Enns,J. B.; Gillham, J. K. The Time-Temperature-Transformation (TTT) Cure Diagram: Modeling the Cure Behavior of Thermosets.(1983). *J. Appl. Polym. Sci.*,Vol. 28, No.8, pp.2567-2591

Fischer, W.; Hofmann, W.; Kaskikallio, J. the Curing Mechanism of Epoxy Resins. (1956). *J. Appl. Chem.*, Vol.6, No.10, pp.429-441

Fischer, W. Polyesters from Expoxides and Anhydrides. (1960). *J. Polym. Sci.*,Vol.44, No.173, pp.155-172

Fornasiero, F.; Olaya, M. M.; Wagner, I.; Brüderle, F.; Prausnitz, M.J. Solubilities of Nonvolatile Solutes in Polymers from Molecular Thermodynamics. (2002). *AIChE J.*, Vol.48, No.6, pp.1284-1291

Gan, W.J.; Yu, Y.F.; Wang, M.H.; Tao, Q.S.; Li, S.J. Viscoelastic Dffects on the Phase Separation in Hermoplastics-Modified Epoxy Resin. (2003). *Macromolecules*, Vol.36, No20, pp.7746-7751

Gillham, K.J. Formation and Properties of Thermosetting and High Tg Polymeric Materials. Polym. Eng. Sci., Vol.26, No.20, 1429-1433

Girard-Reydet, E.; Sautereau, H.; Pascault, J.P.; Keates, P.; Navard, P.; Thollet, G.; Vigier, G. Reaction-Induced Phase Separation Mechanisms in Modified Thermosets. (1998). *Polymer*, Vol. 39, No.11, pp.2269-2279

Girard-Reydet, E.; Vocard, V.; Pascault, P. J.; Sauterau, H. Polyetherimide-Modified Epoxy Networks: Influence of Cure Conditions on Morphology and Mechanical Properties. (1997). *J. Appl. Polym. Sci.*, Vol. 65, No.12, pp.2433–2445

Grillet, A.C.; Galy, J.; Pascault, J.P. Influence of a 2-Step Process and of Different Cure Schedules on the Generated Morphology of a Rubber-Modified Epoxy System Based on Aromatic Diamines.(1992).*Polymer*, Vol.33, No.1, pp34-43.

Halley, J.P＆Mackay, E.M. Chemorheology of Thermosets-An Overview. (1996). *Polym. Eng. Sci.*, Vol. 36, No. 5 pp.693-609

Hedrick, L .J.; Yilgör, I.; Wilkes, L. G.; McGrath, E. J. Chemical Modification Of Matrix Resin Networks with Engineering Thermoplastics.(1985).

Hildebrand, J.H.＆ Scott, R.L. the solubility of nonelectrolytes, 3rd Edition, Reinhold Pub. Co., New York (1950)

Hess, W, Vilgis, A T, Winter, H.H. Dynamical Critical-Behavior during Chemical Gelation and Vulcanization. (1988). *Macromolecules*, Vol. 21, No.8, pp.2536-2542

Hohenberg, C.P.; Halperin, I.B. Theory of Dynamic Critical Phenomena. (1977). *Rev. Mod. Phys.*, Vol.49, No.3, pp.435-479

Hourston,J.D.; Lane, M.J.; Macbeath,A.N. Toughening of epoxy resins with thermoplastics. Ii. Tetrafunctional epoxy resin-polyetherimide blends. (1991). Polymer International,Volum. 26, No 1, pp.17–21

Hwang, W.J; Cho,K; ParK, E.C.; Huh, W. Phase Separation Behavior of Cyanate Ester Resin/Polysulfone Blends.(1999). *J. Appl.Polym. Sc.*, Vol. 74, No.1, pp.33–45

Inoue, T. Reaction-induced Phase Decomposition in Polymer Blends. (1995). Progress Polymer Science, Vol.20, pp.119-153

Kim,B.S.; Chiba, T.; Inoue, T. A New Time-Temperature-Transformation Cure Diagram for Thermoset/Thermoplastic Blend: Tetrafunctional Epoxy/Poly(Ether Sulfone).(1993). *Polymer*, 1993, Vol. 34, No.13, pp. 2809-2815

Kim, M.; Kim, W.; Youngson, Choe, Y.S; Park, M.J.; Park, S.I. Characterization of Cure Reactions of Anhydride/ Epoxy/Polyetherimide Blends.(2002). *Polym. Int.*, Vol.51, No.12, pp.1353–1360

Kissinger, H.E. Reaction Kinetics in Differential Thermal Analysis. (1957). *Analytical Chemistry*, Vol.29, No.11, pp.1702-1706

Launey, E. M.; Buehler, J. M.; Ritchie, O. R. on the Mechanistic Origins of Toughness in Bone. (2010). *Annual reviews Materials Research*, Vol.40, p25-53

Lewin, L. J.; Maerzke, A.K; Nathan, E. Schultz, E.N.; Ross, B.R.; Siepmann, I.J. Prediction of Hildebrand Solubility Parameters of Acrylate and Methacrylate Monomers and Their Mixtures by Molecular Simulation.(2010). *J. Appl .Polym. Sci.*, Vol. 116, No.1, pp.1–9

Macosko, C. W.; Millerlb, D. R. A New Derivation of Average Molecular Weights of Nonlinear Polymers (1976). *Macromolecules*, Vol.9, No. 2, pp.199-206

Martuscelli, M; Musto,P.; Ragosta, G. 1996-10-01. *Advanced Routes for Polymer Toughening.* Elsevier Science Publishing Company, ISBN-10 / ASIN: 0444819606. Sara Burgerhartstraat 25, P.O. Box 211,1000 AE Asterdam, the Netherland

Mijovic, J.; Andjelic, S. Study of the mechanism and rate of bismaleimide cure by remote in-situ real time fiber optic near-infrared spectroscopy. (1996). *Macromolecules*, Vol.29, No.1, pp239-246

Montserrat, S.; Flaque, C.; Calafell M.; Andreu G.; Malek J. Influence of the Accelerator Concentration on the Curing Reaction of an Epoxy-Anhydride System. (1995).*Thermochimica Acta*, 269:213-229

Mours, M.&Winter, H.H. Time-Resolved Rheometry. (1994). Rheologica Acta, Vol.33, No.5,pp.385-397

Muthukumar, M. Screening Effect on Viscoelasticity Near the Gel Point. (1989). *Macromolecules*, Vol.22, No.12, pp.4656-4658

Oyanguren, A. P.; Aizpurua, B.; Gaamte, J. M.; Riccardi, C. C.; Cortazar, D. O.; Mondragon, I. Design of the Ultimate Behavior of Tetrafunctional Epoxies Modified with Polysulfone by Controlling Microstructure Development. (1999). *J.Polym. Sci., Part B: Polym. Phys.*, Vol. 37, No.19, pp.2711–2725

Oyanguren, A. P.; Galante, J.M.; Andromaque, K.; Frontini, M.P.; Williams, J.J.R. Development of bicontinuous morphologies in polysulfone–epoxy blends. (1999). Polymer, Vol.40, No.19,pp.5249–5255

Ohnaga, T.; Chen, W.J.; Inoue, T. Structure Development by Reaction-Induced Phase-Separation in Polymer Mixtures - Computer-Simulation of the Spinodal Decomposition under the Non-Isoquench Depth. (1994). *Polymer*, 35(17): pp3774-3781

Onuki,A. Late Stage Spinodal Decomposition In Polymer Mixtures.(1986). *J. Chern. Phys.*, Vol.85, No.2, pp.1122-1125

Onuki, A.; Nishimori, H. Anomalously Slow Domain Growth due to a Modulus Inhomogeneity in Phase-separating Alloys, (1991). *Phys. Rev. B,* Vol.43,No.16, pp 13649-13652

Onuki, A. ; Taniguchi,T. Viscoelastic Effects in Early Stage Phase Separation in Polymeric Systems.(1997). *J. Chem. Phys.* Vol. 106, No.13, pp.5791-5770.

Onuki, A. &Taniguchi, T. Viscoelastic Effects in Early Stage Phase Separation in Polymeric Systems.(1997). J. Chem. Phys., Vol.106, No.13, pp.5761-5770

Oono, Y.; Puri S. Study of Phase-Separation Dynamics by Use of Cell Dynamical Systems. I. Modeling.(1988). *Phys. Rev. A* Vol.38, No.1, pp.434–453

Pearson, R. A.;Yee, A.F. Toughening Mechanisms in Thermoplastic-Modified Epoxies: 1.Modification Using Poly(Phenylene Oxide). (1993). *Polymer*, Vol.34, No.17, pp.3658-3670

Ruccardi, C. C.; Borrajo, J.;Williams, J. J. R.; Cirard-Reydet, E.; Sauterau, H.; Pascault, P.J. Thermodynamic Analysis of the Phase Separation in Polyetherimide-Modified Epoxies.(1996). *J. Polym.Sci., Part B: Polym.Phys.*, Vol. 34, No.8, pp.349-356

Riccardi, C.C.; Bborrajo, J.; Meynie, L.; Fenoulillot, O.F.; Pascault, P.J. Thermodynamic Analysis of the Phase Separation during the Polymerization of a Thermoset System

into a Thermoplastic Matrix. I. Effect of the Composition on the Cloud-Point Curves. (2004). *J. Polym. Sci., Part B: Polym. Phys.*, Vol. 42, No.8, pp.1351–1360

Riccardi C.C.; Bborrajo J.; Meynie L.; Fenoulillot O.F.; Pascault P.J. Thermodynamic Analysis of The Phase Separation During The Polymerization Of A Thermoset System Into A Thermoplastic Matrix. II. Prediction of The Phase Composition And The Volume Fraction Of The Dispersed Phase. (2004). *J. Polym. Sci., Part B: Polym. Phys.*, Vol. 42, No.8, pp.1361–1368

Riccardi, C.C.; Borrajo, J.;Williams, R.J.J. Thermodynamic Analysis of Phase-Separation in Rubber-Modified Thermosetting Polymers - Influence of the Reactive Polymer Polydispersity. (1994). *Polymer*, Vol.35, No.25, pp5541-5550

Ritzenthaler, S.; Court,F.; David, L.; Girard-Reydet, E.; Leibler, L.; Pascault, P.J. ABC Triblock Copolymers/Epoxy-Diamine Blends. 1. Keys To Achieve Nanostructured Thermosets.(2002). *Macromolecules*, Vol.35, No16, pp.6245-6254

Ritzenthaler, S.; Court, F.; David, L.; Girard-Reydet, E.; Leibler, L.; Pascault P.J. ABC Triblock Copolymers/Epoxy- Diamine Blends. 2. Parameters Controlling the Morphologies and Properties.(2003). *Macromolecules*, Vol.36, No.1, pp.118-126

Rozenberg, A.B.; Boiko, G.N.; Morgan, R.J.; Shin, E.E. the Cure J. Mechanism of the 4,4'-(N,N'- bismaleimide) diphenylmethane -2,2'-diallylbisphenol A System. (2001). *Polymer Science Series* A, Vol.43, No.4, pp.386-399

Ruseckaite, R.A.; Hu, L.; Riccardi, C.C.; Williams, R.J.J. Castor-Oil Modified Epoxy Resins as Model Systems of Rubber-Modified Thermosets. 2: Influence of Cure Conditions on Morphologies Generated. (1993).*Polym. Int.*, Vol.30, No.3, pp.287-295

Scanlan, J.C.; Winter, H. H. Composition Dependence of the Viscoelasticity of End-linked Poly(dimethylsiloxane) at the Gel Point.(1991). *Macromolecules*, Vol.24, No.1, pp47-54

Shibahara, S;Yamamoto, T.; Motoyoshiya, J.; Hayashi, S. Curing Reactions of Bismaleimido Diphenylmethane with Mono- or Di-Functional Allylphenols-High Resolution Solid-State C-13 NMR Study. (1998). *Polym. J.*, Vol.30, No.5, pp.410-413

Simon, S.L.; Gillham, J.K. Thermosetting Cure Diagram: Calculation and Application. (1994). *J. Appl. Polym. Sci.*, Vol.53, No.4, pp709-727

Tanaka, H. Viscoelastic Model of Phase Separation. (1997), *Physical Review E.* Vol.56, No.4, pp4451-4462

Taniguchi, T.& Onuki, A. Network Domain Structure in Viscoelastic Phase Separation. *Phys. Rev. Lett.*, Vol. 77, No.24, pp.4910-4913

Utracki L.A.; Simha R. Statistical Thermodynamics Predictions of the Solubility Parameter.(2004). *Polym. Int.*, Vol.53, No.3, pp.279–286

Williams, J. J. R.; Boris A. Rozenberg, A.B.; Pascault, P.J. Reaction-induced phase separation in modified thermosetting polymers. (1997). *Advances in Polymer Science, Polymer Analysis Polymer Physics*, Volm.128, pp.95-156

Wisanrakkit, G.&Gillham, J.K. The Glass Transition Temperature (Tg) as an Index of Chemical Conversion for a High-Tg Amine/Epoxy System: Chemical and Diffusion Controlled Reaction Kinetics. (1990). *J. Appl. Polym. Sci*, Vol.41, No11-12, pp.2885-2929

Xiong, Y.; Boey, F.Y. C.; Rath, K.S. Kinetic Study of the Curing Behavior of Bismaleimide Modified with Diallylbisphenol A. (2003). *J. Appl. Polym. Sci*, Vol.90, No.8, pp.2229-2240

Xu, J.J.; Holst, M.; Rullmann, M.;Wenzel, M.; Alig, I. Reaction-Induced Phase Separation In A Polysulfone-Modified Epoxy-Anhydride Thermoset. (2007). *J. Macromol. Sci. Phys.*, 46(1):155-181

Xu, Y.Z. & Zhang, X.J. Inversed Polarized Hotstage Microscope with High Resolution, Long Working Distance and High Temperature Duration. Chinese Patent. 2007200666499

Yi X.S. (2009). Research, Development and Enhancement of High-performance Polymer Matrix Composites for Aerospace in China.Proceeding of ICCM17, Edinburgh, UK, 27-31 July 2009

Yi X.S. Research and Development of Advanced Composite Materials Technology (in Chinese). National Defense Press, Beijing, 2006

Yi, X.S.; An, X.F.; Tang, B.M.; Pan, Y. Ex-Situ Formation of Periodic Interlayer Structure to Improve Significantly the Impact Damage Resistance of Carbon Laminates. (2003). *Advance Engineering Materials*, Vol.10, No.10, pp.729-732

Yi, X.S.; An, X.F. Developments of High-performance Composites by Innovative Ex situ Concept for Aerospace Application. (2008). *J. Thermoplast. Compos.,*Vol. 22, No.1, pp.29-49

Yi, X.S.; Xu, Y.H.; Cheng, Q.F.; An, X.F. Development of Studies on Polymer Matrix Aircraft Composite Materials Highly Toughened. (2008). *Science & Technology Review*, Vol.26,No.6, pp84-92 ISSN: 1000-7857 CN:11-1421/N

Yu Y.F.; Wang, M.H.; Gan, W.J.; Tao, Q.S.; Li, S.J. Cure Induced Viscoelastic Phase Separation in Polyethersulfone Modied Epoxy System.(2004).*Phys.Chem. E*, Vol.108,pp.6208-621

Zhang, H.D.Theoretical Studies and Computer Simulations of Phase Separation Kinetics of Polymer Mixtures. (1999). Ph. D. Dissertation, Fudan Unversity

Zhang, X.J. the Rheology and Morphology of Thermoplastic Modified Thermoseting Systems. (2008). Ph.D. Dissertation, Fudan University

Zhang, X.J.;Xu, Y.Z. *Proceeding of Advances in Rheology*,2006,138-144, Shandong University Press

Zhang, X.J.; Yi, X.S.; Xu, Y.Z. Cure Induced Phase Separation of Epoxy/DDS/PEK-C Composites and its Temperature Dependency. (2008). *J. App. Polym.Sci.*, Vol.109, No 4, pp2195–2206

Zhang, X.J.; Yi, X.S.; Xu, Y.Z. the Effect of Chemical structure on the Phase Separation Time/temperature Dependence in Thermoplastics Modified Thermosetting Systems.(2008). *Acta Polymeric Sinica*, No.6, pp583-591

Zhang, X.J.;Yi, X.S.; Xu, Y.Z. the Time/temperature Relationship during Phase Separation of Different Thermoplastic Modified Thermosetting Systems. (2007). *Acta Polymeric Sinica*, No 8, pp715-720

Zhang, X.J.; Yi, X. S.; Xu, Y.Z. Rheology and Morphology Development During Phase Separation and Gelation of Phenolphthalein Polyetherketon Modified Epoxy Resins. *Proceeding of the 22th Annual Meeting of the Polymer Processing Society*, pp527. Yamagata, Japan, Polymer Processing Society. July 2-6,2006

Zucchi, A.I.;Galante, J. M.; Borrajo, J.; Williams, J. J. R. A Model System for the Thermodynamic Analysis of Reaction-Induced Phase Separation: Solutions of Polystyrene in Bifunctional Epoxy/Amine Monomers. (2004). *Macromol. Chem. Phys.*, Vol.205, pp676–683

IntechOpen

IntechOpen

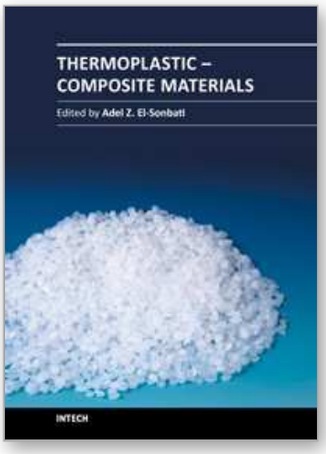

Thermoplastic - Composite Materials

Edited by Prof. Adel El-Sonbati

ISBN 978-953-51-0310-3
Hard cover, 146 pages
Publisher InTech
Published online 16, March, 2012
Published in print edition March, 2012

Composite materials often demand a unique combination of properties, including high thermal and oxidative stability, toughness, solvent resistance and low dielectric constant. This book, "Thermoplastic - Composite Materials", is comprised of seven excellent chapters, written for all specialized scientists and engineers dealing with characterization, thermal, mechanical and technical properties, rheological, morphological and microstructure properties and processing design of composite materials.

How to reference

In order to correctly reference this scholarly work, feel free to copy and paste the following:

Yuanze Xu and Xiujuan Zhang (2012). High Performance Thermoplastic/Thermosetting Composites Microstructure and Processing Design Based on Phase Separation, Thermoplastic - Composite Materials, Prof. Adel El-Sonbati (Ed.), ISBN: 978-953-51-0310-3, InTech, Available from: http://www.intechopen.com/books/thermoplastic-composite-materials/high-performance-thermoplastic-thermosetting-composites-structure-processing-design-based-on-phase-s

INTECH
open science | open minds

InTech Europe
University Campus STeP Ri
Slavka Krautzeka 83/A
51000 Rijeka, Croatia
Phone: +385 (51) 770 447
Fax: +385 (51) 686 166
www.intechopen.com

InTech China
Unit 405, Office Block, Hotel Equatorial Shanghai
No.65, Yan An Road (West), Shanghai, 200040, China
中国上海市延安西路65号上海国际贵都大饭店办公楼405单元
Phone: +86-21-62489820
Fax: +86-21-62489821

© 2012 The Author(s). Licensee IntechOpen. This is an open access article distributed under the terms of the Creative Commons Attribution 3.0 License, which permits unrestricted use, distribution, and reproduction in any medium, provided the original work is properly cited.